2020

The Purification and Characterization of N-terminally Acetylated Ssal from Saccharomyces cerevisiae

Alijah A. Griffith

The purification and characterization of N-terminally acetylated Ssa1 from *Saccharomyces cerevisiae*

An undergraduate project presented
By Alijah A. Griffith
To the Biology Department

Faculty Advisor: William Holmes, Ph.D.

The purification and characterization of N-terminally acetylated Ssa1 from *Saccharomyces cerevisiae*

By Alijah A. Griffith

A Thesis Submitted in Partial Fulfillment of
the Requirements for the Degree of

Bachelor of Science
in the
Department of Biology Honors

The Faculty of Arts and Sciences
Rhode Island College
2020

APPROVED:

_____	_____
Name, Faculty Advisor	Date
_____	_____
Name, Honors Committee Chair	Date
_____	_____
Name, Department Chair	Date

Abstract

Molecular chaperones are highly conserved, ubiquitous enzymes that maintain proteostasis by mediating protein structure *in vivo*. Post-translational modifications (PTMs) can act as a functional switch between chaperone pathways, allowing for cells to enact a coordinated response to cellular perturbations. Several PTMs are well-characterized in the context of chaperone function, though the role of N-terminal acetylation is commonly overlooked, leading to an overwhelming lack of scientific understanding in this area of study. Ssa1, a Hsp70 class chaperone endogenous to *Saccharomyces cerevisiae*, is likely N-terminally acetylated, though *in vitro* studies of Ssa1 are limited by current purification methods which are resource-intensive. To address these limitations, we developed a one-step purification scheme that uses a Protein-A fusion transformant strain in combination with IgG-conjugated magnetic Dynabeads to facilitate Ssa1 pull-down. Using this method, Ssa1 was natively isolated in high purity and yield while retaining its activity and our modification of interest. This study also established the basis for evaluating differences Ssa1 chaperone activity due to disruption of N-terminal acetylation by purifying Ssa1 in N-terminal acetylation deficient backgrounds. Through the expression and purification of the Ssa1 co-chaperone, Ydj1, this study has additionally provided components needed to facilitate future co-chaperone binding experiments, which will help determine the contribution of N-terminal acetylation to Hsp70 chaperone activity and efficiency.

Table of Contents

Introduction

The majority of proteins expressed in cells must achieve a specific, highly defined three-dimensional structure, known as the native state, to execute proper enzymatic function (Petrescu et al. 2000; Klaips et al. 2018; Turoverov et al. 2010). The native state is dictated by the amino acid sequence of a given protein (Anfinsen, 1973), though now, the native state considered a designation of function rather than of structural character (Turoverov et al. 2010). The conceptual redefinition of native state is attributable to the discovery that several proteins retain their biological function while exhibiting notable structural disorder. Regardless of structural disorder, the majority of eukaryotic proteins require the assistance of chaperone proteins to assume their respective native conformations efficiently and within a biologically relevant timescale (Klaips et al. 2018).

Since their initial discovery, several families of chaperone proteins were identified across all domains of life, illustrating their highly conserved functional role in maintaining proteostasis. Molecular chaperones and their regulatory cofactors both mediate and coordinate the processes of protein synthesis, protein folding, conformational maintenance, and protein degradation (Klaips et al. 2018). In doing so, molecular chaperones prevent protein misfolding, aggregation, and the accumulation of toxic protein species (Kellner et al. 2014; Vjestica et al. 2013; Klaips et al. 2018) that is characteristic to several diseases linked to aberrant protein folding (Lee et al. 2013; Barral et al. 2004). Continued study indicates that post-translational modifications (PTMs) likely regulate alternative chaperone function (Griffith and Holmes, 2019).

Accordingly, the effects of PTMs on chaperone activity have become of increasing interest to both scientific and medical fields.

PTMs are known to be of critical importance to the efficiency of Hsp70 chaperones. Hsp70 chaperones are the most evolutionarily conserved family of chaperone proteins, with the number of isoforms expressed increasing with organismal complexity (Gupta et al. 1993, Boorstein et al. 1994). Hsp70s exhibit extreme functional diversity and are able found to interact with a wide variety of client substrates within all major intracellular compartments (Gupta et al. 1993; Boorstein et al. 1994). Hsp70 expression was traditionally characterized as inducible because of their initial discovery under conditions of thermal stress, though it is now recognized that Hsp70s are also expressed constitutively (Lindquist and Craig, 1988).

Organelle-associated Hsp70s are typically encoded by a single gene in the majority of organisms; conversely, cytoplasmic Hsp70s are usually encoded by a series of homologous genes. In *Saccharomyces cerevisiae* (yeast), there are at least fourteen identified Hsp70 isoforms, which are further categorized into five subclasses according to amino acid sequence identity conservation (Boorstein et al. 1994). Only two subclasses, Ssa and Ssb, exhibit a cytoplasmic distribution, with the expression of members of the Ssa subclass considered essential for cell viability (Boorstein et al. 1994)

It is well established that Hsp70 chaperones are subject to several PTMs. PTMs modify the biochemical characteristic of specific amino acid side chains, resulting in the modified protein exhibiting both an altered form and dynamic, which serves to increase proteomic diversity (Truman et al. 2012; Morgner et al. 2015).To date the roles of several PTMs, including phosphorylation and lysine acetylation, have been characterized in the

context of Hsp70 activity; however, the role of N-terminal acetylation in Hsp70 chaperone function remains comparatively limited (Griffith and Holmes, 2019).

N-terminal acetylation is a PTM that leads to proteomic diversity through the constitution of a cellular acetylome, wherein N-terminally acetylated proteins exhibit an alternate function and dynamic, subsequently allowing cells to react specifically to environmental stressors or cellular perturbations by various intracellular signaling pathways. N-terminal acetylation is catalyzed by a collection of N-terminal acetyltransferases (NATs), which transfer acetyl moieties from acetyl-coenzyme A to α-amino groups at specific N-terminal residues. One theoretical target of N-terminal acetylation is Ssa1, a member of the Ssa subclass of Hsp70 chaperones that are endogenous to *S. cerevisiae*. As an Hsp70 chaperone, Ssa1 works in tandem with its co-chaperones, to maintain cellular proteostasis by restoring the native conformations of misfolded proteins via a transient, ATP-driven mechanism.

There are several factors that implicitly hinder the study of Ssa1, though one of the most limiting factors is its purification. Purifying Ssa1 is often both a resource-intensive and time-consuming process, requiring expensive technologies and large starting volumes of culture to obtain a satisfactory yield.

To facilitate studies that further probe the functional and mechanistic changes associated with the N-terminal acetylation of Ssa1, we developed an efficient, user-friendly, one-step purification method. Our method uses previously transformed strains expressing Protein-A-tagged Ssa1 in combination with IgG-conjugated magnetic Dynabeads to facilitate pull-down without disrupting our modification of interest . Our results indicate that our method is able to natively isolate high yields of pure acetylated

and unacetylated Ssa1 without compromising enzymatic activity, allowing for future investigation of the effects of N-terminal acetylation on Hsp70 function and dynamic.

Molecular Chaperones

To maintain proteostasis, cells utilize the coordinated action of molecular chaperones to preserve the appropriate synthesis, folding, conformation, and degradation of target proteins (Jayark et al. 2020). The amino-acid sequence of any given protein, encoded in genomic DNA, dictates its native conformation. This fact exemplified by the ability of small proteins re-fold (within a microsecond timescale) without assistance when removed from denaturant *in vitro* (Hartl et al. 2011). This is a considerably more difficult feat for multi-domain proteins, which often requires several minutes to hours to achieve their respective native states, if even possible (Hartl et al. 2011). *In vivo* conditions further complicate protein folding due to macromolecular crowding within the cytosol, increasing the tendency of non-native and conformationally flexible proteins to aggregate (Hartl et al. 2011). By preventing aberrant intermolecular interactions and lowering entropic costs, chaperone proteins minimize protein aggregation, maintain protein solubility, and promote protein refolding (Griffith and Holmes, 2019).

Chaperone proteins are best described as proteins that interact, stabilize, or assist a substrate protein in acquiring its native conformation without being present in its final structure (Hartl FU, 1996; Hartl et al. 2001). Traditionally, chaperone proteins are categorized within families. Though structurally unrelated, members of chaperone families are often referred to as heat-shock proteins (Hsps) due to their induction under thermal stress and are classified according to molecular weight in kDa (Hartl et al. 2001).

sHsps

Small heat shock proteins (sHsps) are a diverse chaperones chaperone family that is expressed in all domains of life (Liu et al. 2015; Jaya et al. 2009; Uji et al. 2019). The number of genes encoding sHsps increases with organismal complexity. Bacteria, Archaea, and unicellular eukaryotes usually possess one or two genes encoding sHsps, while multicellular eukaryotes may contain several, reaching 19 in *Arabidopsis thaliana* and 10 in humans (Żwirowski et al. 2017; Uji et al. 2019). Among the Hsps, the low-molecular-weight sHsps (12-43-kDa) are the most strongly upregulated under stress conditions, when they may constitute >1% of the total cell protein concentration in certain cell populations (Liu et al. 2015; Rutsdottir et al. 2017; Uji et al. 2019). sHsps are known interact with a wide variety of substrates, and consequently have roles in several physiological processes including cell proliferation, cell differentiation, and cytoskeletal organization, among others (Giese et al. 2005; Uji et al. 2019).

Generally, sHsps identify and bind to aggregation-prone, partially unfolded substrates, acting to stabilize and promote a refolding-competent state in an ATP-independent manner (Liu et al. 2015, Giese et al. 2005; Cashikar et al. 2005; Uji et al. 2019). While this is ongoing, ATP-driven chaperones, namely Hsp70 and Hsp100, will together rescue and restore the native conformation of the substrate initially bound by the sHsp (Liu et al. 2015, Giese et al. 2005; Cashikar et al. 2005; Uji et al. 2019; Żwirowski et al. 2017; Peschek et al. 2013). A striking feature of sHsps is assembly into oligomeric complexes, ranging from the inclusion of 12 to over 24 subunits (McLoughlin et al. 2016). While oligomerized, sHsps preserve quaternary structure, which limits their ability

to interact with substrates (Liu et al. 2015; Poulain et al. 2010). Notably, the equilibrium between the oligomeric and smaller sHsps species shifts under increased temperatures, with sHsps assuming a dimeric formation that promotes binding of exposed hydrophobic patches belonging to partially misfolded proteins (Żwirowski et al. 2017).

Monomeric sHsps contain a signature α-crystallin domain (ACD) that is bordered by a variable-length N-terminal region (NTR) and a short C-terminal region (CTR) (Rutsdottir et al. 2017; McLoughlin et al. 2016). The ACD is a conserved C-terminal domain that acts as supportive structure within the sHsp (Cashikar et al. 2005; Rutsdottir et al. 2017), while the CTR directly contributes to sHsps oligomerization by the presence one of the following conserved motifs, I-X-I, I/V-X-I, I-X-I/S, or I/V-X-I/V (Rutsdottir et al. 2017, Poulain et al. 2010). The N-terminal region (NTR), which facilitates substrate binding, often varies in composition between sHsps, likely contributing to differences in substrate specificity between different sHsps (Rutsdottir et al. 2017).

Hsp90

Hsp90s are both a highly conserved and ubiquitous chaperone family that exist in all living domains except Archaea (Johnson et al. 2009; Sullivan et al. 1997; Hoter et al. 2018). Hsp90s can constitute ≤ 2% of mammalian proteins present under non-stress conditions (Johnson et al., 2009; Sullivan et al. 1997; Hoter et al. 2018), and it is known that the expression of at least one isoform is required for eukaryotic viability (Johnson et al. 2009). Hsp90 function is ATP-dependent, requiring the association of Hsp70, Hsp40, and other co-chaperones (Johnson et al. 2009; Prodromou et al. 1997). In eukaryotic cells, cytosolic Hsp90s interact with specific client proteins that are involved in several

cellular processes including signal transduction, cell cycle regulation, cell viability, cell differentiation, apoptosis, adaptive immunity, and hormone responsiveness (Prodromou et al. 1997; Hoter et al. 2018). The additional co-chaperones that may be affiliated with the Hsp90-70-40 complex are shown to be dependent on the identity of the client protein (Prodromou et al. 1997).

Twelve Hsp90 co-chaperones are observed in *S. cerevisiae*, all of which are present as homologs in mammalian cells, though mammals have additional co-chaperones that are not otherwise present in yeast (Johnson et al. 2009 While the specific functions of Hsp90 co-chaperones remain unknown, though their association to Hsp90 can either be spontaneous or may require the binding of ATP to the Hsp90 NTD for successful association (Sullivan et al. 1997; Prodromou et al. 2000). Mutations of the Hsp90 N-terminus which prevent ATP binding are known to alter co-chaperone binding (Prodromou et al. 2000).

The overall molecular structure of Hsp90 comprises three conserved domains, the ATPase N-terminal domain (NTD), the C-terminal domain (CTD), and the middle domain (MD) (Hoter et al. 2018). Eukaryotic Hsp90s also include a flexible charged linker domain (CR) between the NTD and MD, which was shown to be essential for chaperone function, client interaction, and conformational flexibility (Hoter et al. 2018).

Under physiological conditions, Hsp90 typically exists as a homodimer, though when dimerized, Hsp90 assumes a molecular clamp conformation that allows for substrate interaction (Hoter et al. 2018). Hsp90 dimerization is regulated by the NTD and occurs by interaction of CTDs via conserved MEEVD or KDEL motifs, the presence of which are isoform and cellular localization dependent (Prodromou et al. 2000; Hoter et

al. 2017). Co-chaperone binding occurs in the NTD, MD, and CTD, though client protein binding occurs primarily in the MD and CTD (Hoter et al. 2018). When ATP is bound, Hsp90 exhibits a conformation that exhibits decreased substrate affinity by means of decreasing the overall hydrophobicity of the chaperone. Assuming this low-affinity conformation, Hsp90 is able to bind and stabilize client proteins in substantially folded states (Prodromou et al. 2000).

Hsp100

Hsp100 chaperones, or Clp proteins, belong to the AAA+ family of ATP-dependent molecular chaperones (Zeymer et al. 2013; Krzewska et al. 2001). Generally, Hsp100s promote the disassembly of protein aggregates, though specific members can also convey cellular thermotolerance or act as subunits of ATP-dependent proteases (Krzewska et al. 2001). There are two classes of monomeric Hsp100s that are designated by the number of NBDs (nucleotide binding domains) present. Class I Hsp100 chaperones have two NBDs, while class II chaperones contain a single NBD (Lee et al. 2003; Xeymer et al. 2013). When not present in a monomeric state, Hsp100s typically oligomerize into hexameric ring complexes.

Of the Hsp100s, Hsp104 is especially notable for its essential role in conveying thermotolerance in *S. cerevisiae* (Okuda et al. 2015). While there are prokaryotic homologs of Hsp104, such as ClpB in *Escherichia coli,* a mammalian equivalent has not been identified (Okuda et al. 2015; Vacher et al. 2005). When acting in cooperation with the Hsp70/40 chaperone system, Hsp104 solubilizes aggregates in a multistep fashion (Okuda et al. 2015). The protein aggregates are initially bound by an Hsp70/40 complex,

which then recruits Hsp104/ClpB (Okuda et al. 2015). Once recruited, Hsp104/ClpB uses the hydrolysis of ATP to thread the aggregate through the central pore of its hexameric ring, promoting reactivation and solubilization of the aggregates (Okuda et al. 2015; Weibezahn et al. 2004).

Hsp70

Hsp70 chaperones associate with client proteins during the early stages of the folding process (Jana et al. 2009). Hsp70s are capable of acting dynamically and may promiscuously associate to aberrantly folded substrates or preferentially binding to folded substrates (Laufen et al. 1999; Umehara et al. 2018; Rosenzweig et al. 2019). Hsp70s are the most evolutionarily conserved protein known and are expressed in all organisms (Daugaard et al. 2007). The conserved nature of Hsp70 is reflected structurally, as the prokaryotic Hsp70, DnaK, shares 50% amino acid identity with eukaryotic Hsp70s (Daugaard et al. 2007). Furthermore, Hsp70 exhibits extreme functional conservation, as demonstrated by its ability to complement chaperone action both *in vitro* (Jäättelä et al. 1992; Li et al. 1990) and via its transgenic expression (Li et al. 1990; Pelham HR, 1984).

Hsp70s have a universal structure comprised of a N-terminal 44-kDa ATPase nucleotide binding domain (NBD) and an 18-kDa C-terminal substrate-binding domain (SBD), which interacts with short hydrophobic regions of client proteins (Kellner et al. 2014; Taneva et al. 2010; Lui et al. 2007; Mayer and Kityk, 2015; Sharma et al. 2009). The NBD contains four subdomains which are further separated into two lobes (I and II) by an intervening central ATP binding pocket. The SBD contains a two-layered β-sandwich domain (SBDβ) that surrounds the substrate binding site, an α-helical lid

domain (SBDα), which shields the SBD when the chaperone assumes a closed conformational state, and an intrinsically disordered region present at the extreme C-terminus (C-IDR) (Gong et al. 2018; Zhang et al. 2014). Notably, the C-IDR contains an EEVD motif and a GGAP motif which promotes co-chaperone and substrate recognition, respectively (Gong et al. 2018; Zhang et al. 2014). Notably, the substrate diversity of Hsp70 is due to the degenerative recognition motif within the SBDβ, which features an amino acid composition that is highly advantageous for client binding (Jaya et al. 2009; Rüdiger et al. 1997).

The NBD and SBD domains are connected by a highly conserved interdomain linker, which is largely hydrophobic and allosterically coordinates the respective domains, which is essential for Hsp70 function (Umehara et al. 2018; Zhang et al. 2014). Interdomain allosteric communication allows proper Hsp70 function via the cycling between two main conformations, as dictated by the inherent ATPase activity of the chaperone (Jana et al. 2009). When ATP is bound within the NBD, Hsp70 assumes an open conformation which exhibits a low substrate affinity along with high rates of substrate association and dissociation (Rippmann et al. 1991; Shorter et al. 2008; Abrams et al. 2014; Mayer and Kityk, 2015). Conversely, ATP hydrolysis promotes a closed conformation, which displays a 100- and 1000-fold decrease in substrate on/off rates, respectively, and a 10- to 50-fold increase in substrate affinity (Rippmann et al. 1991; Abrams et al. 2014; Shorter et al. 2008; Mayer and Kityk, 2015). The reiteration of these two conformations ultimately result in the promotion of the substrate to its natural state (Abrams et al. 2014).

The regulatory mechanisms underlying Hsp70 allostery remain to be characterized, though the conformational cycling by which Hsp70 facilitates substrate refolding is regulated by nucleotide binding, substrate identity, Hsp40 co-chaperones, and nucleotide exchange factors (NEFs), respectively. Both the association of Hsp40s, which coordinate Hsp70 ATP-ase activity with substrate binding, and NEFs, including the members of the GrpE, Snl1 (Bag-1), Sse1/Sse2 (Hsp110), Fes1 (HspBp1) families, which expedite nucleotide exchange, greatly enhance chaperone efficiency (Abrams et al. 2014; Mayer and Kityk, 2015; Sharma et al. 2009; Ngosuwan et al. 2003).

Hsp40s and NEFs

When acting in concert with members of the Hsp70 family, Hsp40s target Hsp70s to specific substrates by modulating Hsp70 ATPase activity and stabilizing Hsp70-polypeptide complexes (Vjestica et al. 2013; Lu and Cyr. 1998; Laufen et al. 1999). Hsp40 activity is essential for Hsp70 efficiency though the mechanism by which Hsp40 chaperones target Hsp70s to substrates is not yet known (Fan et al. 2005). Hsp40 members exhibit unique combinations of four characteristic domains that were initially described in the prototypic DnaJ endogenous to *Escherichia coli* : the J-domain, a C-terminal peptide fragment, a G/F-rich containing region, and a zinc finger-like domain (Lu and Cyr, 1998; Greene et al. 1998; Hu et al. 2008). Conservation across the four characteristic domains occurs only in a small selection of Hsp40s; therefore, Hsp40s are categorized into three subtypes according to their domain composition. Only Type I Hsp40s, including Ydj1 in *S. cerevisiae* and Hdj2 in humans, share all four canonical domains with DnaJ (Hu et al. 2008; Kityk et al. 2018; Cheetham et al. 1994; Cyr and

Douglas, 1994). Overall, the J-domain, a helical harpin structure (70-75 residues), is the most conserved of the Hsp40 domains (Kityk et al. 2018; Lu et al. 1998; Cheetham et al. 1994; Wall et al. 1995). Additionally, the J-domain contains the signature HPD motif which is responsible interacting with Hsp70 and regulating the ATPase activity of Hsp70, modulating substrate binding (Fan et al. 2005; Misselwitz et al. 1998; Sha et al. 2000)

Conversely, NEFs, which bind to the Hsp70 NBD, hasten the process of nucleotide exchange (Abrams et al. 2014). Four families of NEFs are known to interact with Hsp70: GrpE, Sse1/Sse2 (Hsp110), Fes1 (HspBp1), and Snl1 (Bag-1); the last three have homologs present in humans (Abrams et al. 2014). Overall, each NEF family is structurally distinct and varies from one another in terms of general mechanism, interaction, and affinity for Hsp70 (Abrams et al. 2014; Sondermann et al. 2001).

Molecular chaperones in disease and treatment

The medical relevance of protein folding is considerable. A number of human diseases, including the classic examples of Alzheimer's disease (AD) and cystic fibrosis (CF), are now suggested to result from aberrant protein folding (Barral et al. 2004). While there are various mechanisms by which aberrant protein folding contributes to cellular dysfunction, it is evident that chaperone proteins play an increasingly direct role in protein-folding diseases. Consequently, the overall contribution of chaperone proteins to disease onset and their potential as therapeutic targets have become subjects of increased study.

To date, several inheritable diseases have been linked to mutations occurring in chaperone-encoding genes. There are too many examples to discuss extensively within

this body of work; however, this point is easily exemplified by the study of α-crystallins, a well-known sHsp (Barral et al. 2004; Jaya et al. 2009; Giese et al. 2005). In humans, α-crystallin is composed of two subunits, αA and αB, both encoded by separate genes (Barral et al. 2004). Missense mutations of a conserved arginine residue within the core domains of each subunit implicated in the onset of human disease. The R120G in αB-crystallin results desmin-related myopathy (DRMs) (Ojha et al. 2010; Treweek et al. 2005), while the R116C mutation in αA-crystallin results in hereditary cataracts (Litt et al. 1998).

αA-crystallin is a major cytosolic constituent of the lens within the eye. While it is not well understood how R116C αA-crystallin affects lens opacity, it is likely that the inability of αA-crystallin to promote the folding of other major lens proteins leads to the precipitation of β- and γ-crystallin and subsequent cataract formation (Litt et al. 1998; Barral et al. 2004). Conversely, αB-crystallin interacts desmin protein within skeletal muscle cells and is suggested to promote either folding or intermediate filament assembly (Djabali et al. 1997; Barral et al. 2004).

Hsp90 is also known to contribute to several pathologies, though most notably Parkinson's disease (PD). PD is a neurodegenerative disorder that is characterized by bradykinesia, rigidity, resting tremors, the loss of dopaminergic neurons in the *substantia nigra* and the formation of Lewy bodies in patients (Wang et al. 2008). Some inherited cases of PD are the result of a toxic gain of function in leucine-rich repeat kinase 2 (LRRK2), which normally complexes with Hsp90 (Wang et al. 2008).

The importance of Hsp70 chaperones in disease is impossible to overlook (Barral et al. 2004), especially polyglutamate expansion diseases. To date, at least eight inherited

human neurodegenerative diseases are linked to polyglutamate expansion, including Parkinson's disease, prion diseases, and Alzheimer's disease (Magrane et al. 2004). Polyglutamine domain expansion promotes protein toxicity, dysfunction, and neuronal loss, promoting aggregation and formation of ubiquinated nuclear inclusions (NI) (Warrick et al. 1999). Though while chaperone proteins contribute to disease, it is increasingly apparent that Hsps are of notable importance in devising novel treatments. For example, on a *Drosophila melanogaster* model of polyglutamine disease, directed expression of Hsp70 suppressed polyglutamine-induced neurodegeneration *in vivo,* indicating that Hsp70 may provide a means of treatment (Warrick et al. 1999).

Another example is found in the transgenic expression of Hsp27, which was determined to reduce cortical damage after cerebral ischemia through mediating cell death in mice (van der Weerd et al. 2009). Similarly, the use of Hsp90 inhibitors promotes the degradation of mutant LRRK2 by blocking the disassociation of Hsp90-LRRK2, establishing a potential route of treatment for PD (Wang et al. 2008).

Overall, it is clear that modulating chaperone function holds incredible therapeutic potential thought it is worthwhile to also consider the role of post-translational modification (PTMs) in both disease pathology and altered chaperone function. PTMs occur in response to dynamic cellular conditions and are catalyzed by highly specialized enzymes. Several PTMs, including phosphorylation, methylation, and acetylation involve the covalent addition of small functional groups to target proteins at specific residues, though macromolecules, including carbohydrates and lipids, may also be used to modify target substrates.

It is well known that PTMs can act as a functional switch between different chaperone pathways by altering chaperone binding to both clients and co-chaperones; however, the role of N-terminal acetylation in chaperone function is commonly overlooked, leading to an overwhelming lack of scientific understanding in this area of study.

N-terminal acetylation

N-terminal acetylation is an irreversible protein modification in which an acetyl moiety is transferred from acetyl-coenzyme A (Ac-CoA) to the α-amino group of a polypeptide chain (Polevoda et al. 1999). N-terminal acetylation increases proteomic diversity by constituting an intracellular "acetylome," wherein N-terminally acetylated proteins exhibit altered function and provide the basis for cell signaling, allowing a given cell to react specifically to perturbation. The prevalence of N-terminal acetylation in eukaryotes is undebatable as approximately 85.0% of eukaryotic cellular proteins have been shown to be N-terminally acetylated by global analyses (Arnesen et al. 2009; Polevoda et al. 2000.; Polevoda et al. 1999). Notably, the modification occurs rarely, if at all, in Archaea and Bacteria (Arnesen et al. 2009; Polevoda et al. 2000.; Polevoda et al. 1999), which is in agreement with the frequency of N-terminally acetylated proteins occurring in accordance with organismal complexity (Polevoda et al. 1999; Arnesen et al. 2009). While N-terminal acetylation constitutes a complex regulatory system in eukaryotes, the physiological consequence of N-terminal acetylation remains to be understood.

NAT Complexes

N-terminal acetylation is catalyzed by a collection of enzymes known as N-terminal acetyltransferases (NATs). As mentioned previously, NATs catalyze the transfer of acetyl functional groups from acetyl-coenzyme A to the α-amino group at the N-terminal residues, neutralizing the positive charge of the residue and barring further modification of the N-terminus (Kontaxi and Piccardo, 2017; Polevoda et al. 2002). While referred to generally as a PTM, N-terminal acetylation occurs co-translationally when ≥ 20 residues extrude from the ribosome (Kontaxi and Piccardo, 2017; Polevoda et al. 2002).Because N-terminal acetylation is not dependent on the identity of a single residue, the N-terminal sequences subject to this modification exhibit high sequence diversity. Consequently, attempts to predict the likelihood of N-terminal acetylation on the basis N-terminal residue identity are largely ineffective (Helbig et al. 2010). Most of the current insights concerning the NAT complex specificity are credited to knockout studies performed in yeast. It is now known that NATs exhibit highly characteristic substrate specificities that depend on the identity of multiple residues, typically those present in the P2 and P3 positions (Singer and Shaw, 2003). Collectively, serine, alanine, methionine, glycine, and threonine constitute over 95% of N-terminally acetylated residues observed in eukaryotic organisms (Polevoda and Sherman, 2000; Polevola et al. 1999).

NATs are part of the GCN5 (general control non-derepressible 5)-related acetyltransferase (GNAT) superfamily (Coleman et al. 1996). Characteristic to the GNAT superfamily, all NATs contain the conserved motif, Q/RxxGxG/A, which is responsible for binding of acetyl-CoA (Coleman et al. 1996). While NATs can exist in monomeric

states, they typically function in multimeric complexes that consist of one major subunit, which dictates both substrate specificity and catalytic activity, and up to two auxiliary subunits, which have varied functions (Liszczak et al. 2013).

To date, six different NAT complexes (NatA-F) are currently described in mammals, though NatA-E are also observed in *S. cerevisiae* (Arnesen et al. 2009; Forte et al. 2011). Approximately 50% of the yeast proteome is proposed to be N-terminally acetylated by the collective action of NatA, NatB, and NatC, along with their respective catalytic subunits, Ard1, Nat3, and Mak3 (Pezza, et al. 2009; Arnesen et al. 2009; Aksnes et al. 2015; Gautschi et al. 2003; Singer and Shaw, 2003).

In terms of substrate specificity, NatA acetylates alanine, glycine, threonine, and serine residues exposed by methionine cleavage (Gautschi et al. 2003; Arnold, et al. 1999), while NatB targets methionine residues for acetylation when they are followed by either alanine, glutamine, asparagine, or methionine at the P2 position (Forte et al. 2011; Polevoda et al. 2003). While thought to be influenced by other sequence elements, NatC acetylates methionine residues adjacent to either isoleucine, leucine, tryptophan, or phenylalanine at P2 (Forte et al. 2011; Polevoda, 2001). Of the NAT complexes, NatD appears to be more specialized, catalyzing the N-terminal acetylation of histones, while NatE only acetylates substrates with leucine at P3 and proline at P4 (Forte et al. 2011).

NatA

NatA is comprised of two main subunits: its adaptor subunit, Nat1, and its catalytic subunit, Ard1, a GNAT homologue which recognizes a wide range sequences, allowing for a diverse collection of appropriate substrates. (Eiyama et al. 2015; Gautschi

et al. 2003) The genes encoding the respective NatA subunits were first suggested by nat1- and ard1- mutants, which lacked NAT activity and exhibited the similar pleiotropic phenotypes of slow growth, temperature sensitivity, failure to enter G_0, and failure to sporulate (Mullen et al. 1989). In the same study, the co-linear functionality of Nat1 and Ard1 was further emphasized through a 20-fold increase in NAT activity, reported only when both genes were overexpressed (Mullen et al. 1989). Subsequent studies have since confirmed that both NatA subunits are essential for activity, as single mutants were unable to execute N-terminal acetylation of characteristic substrates *in vivo* (Mullen et al. 1989; Polevoda et al. 1999; Arnesen et al. 2005). It is proposed that a third subunit, Nat5, may also be present in NatA complexes. While the function of Nat5 is unknown, single deletion mutants for either Ard1 or Nat5 exhibited nearly identical phenotypes, exhibiting slow growth, temperature and salt sensitivity, and osmotic sensitivity, among others (Geissenhoner et al. 2004).

Nat1, the non-catalytic NatA subunit, mediates the stable interaction of the NatA complex with the large ribosomal unit and promotes association with nascent polypeptides of approximately 50 to 80 amino acids in length (Gautshi et al. 2003). Tetratricopeptide repeat (TPR) motifs within Nat1 likely mediate this interaction (Gautshi et al. 2003; Blatch, G.L., Lassle, M. 1999), guiding the nascent polypeptide to the catalytic subunit, Ard1, and the functionally undefined subunit, Nat5, allowing for N-terminal acetylation to occur (Gautshi et al. 2004; Geissenhoner, et al. 2004).

NatB

NatB is composed of one catalytic and one auxiliary subunit, requiring both subunits for it activity (Van Damme et al. 2012; Polevoda et al. 2003; Ametzazurra et al. 2008). Nat3, the 22-kDa catalytic subunit of NatB, was first identified by DNA sequence alignment, wherein it was determined that while sequence similarity to other Nat subunits was limited overall, Nat3 contained several motifs that of high sequence similarity (Polevoda et al. 1999; Coleman et al. 1996). Most notably, residues 144-149 of Nat3 resembled the acetyl-CoA binding motif of the GNAT superfamily, Q/RxxGxG/A, allowing for the function of the subunit to be deduced and later confirmed (Polevoda et al. 1999; Coleman et al. 1996).

In contrast, the 93-kDa subunit, Mdm20, exhibits no homology to previously characterized proteins (Hermann, et al. 1997). Mdm20 was initially identified as a protein essential for tropomyosin-F-actin interaction, though it was later determined that Mdm20 complexes Nat3 to acetylate substrates, including tropomyosin 1 (Tmp1p) (Caesar et al. 2005). While both subunits are required for NatB activity, subsequent work demonstrated that single knockout strains for each subunit displayed many distinctive phenotypes relating to stress resilience and when challenged to grow under minimal media (Caesar et al. 2005). NatB may play regulatory role in the cell cycle, as bioinformatic analyses revealed a notable overrepresentation of proteins involved in cell cycle regulation and DNA processing among NatB substrates (Caesar et al. 2005). Notably, such an observation was not made for NatA or NatC knockouts, which failed to display significant phenotypic differences upon knockout of functional subunits (Caesar et al. 2005).

NatC

NatC is responsible acetylates of polypeptides with Met-Ile, Met-Leu, Met-Trp, and Met-Phe N-termini, although other sequence elements are thought to influence processing as well (Polevoda et al. 2001; Forte et al. 2011). In contrast to other NAT complexes, not much is known about the NatC complex or its targets (Wenzlau et al. 2006). NatC acetyltransferases contain three subunits: the catalytic subunit, Mak3, and auxiliary subunits, Mak10 and Mak31 (Polevoda et al. 2001). All three subunits are required for catalytic activity, as the deletion of any subunits results in abnormal, pleiotropic phenotypes, including the inability to acetylate NatC substrates *in vivo*, and diminished growth under stress conditions or while in minimal media (Polevoda et al. 2001).

Implications of N-Terminal Acetylation

Overall, N-terminal acetylation is thought to be important to many cellular and molecular processes, but its definitive purpose is debated (Van Damme et al. 2011; Lee et al. 1989). Most often, N-terminal acetylation is associated with its role in the N-end rule pathway and ubiquitin-mediated proteolysis (Persson et al. 1985; Hershko et al. 1984; Hwand et al. 2010).

The N-end rule pathway regulates the half-life of a protein by the specific targeting of degradation signals, N-degrons, which promotes polyubiquitination and subsequent degradation of the targeted protein (Shemorry et al. 2013; Varshavsky, A. 2011; Kim et al. 2014). Together, the complimentary nature of N-end rule pathway and

ubiquitin-mediated proteolysis enables the degradation of a majority of cellular polypeptides, which in turn mediates a legion of physiological functions (Varshavsky, A., 2011).

In addition to mediating protein degradation, N-terminal acetylation also holds key roles within cellular differentiation, viability, metabolism and proliferation, protein translocation, membrane attachment, and protein complex formation (Van Damme et al. 2014). Unsurprisingly, because of its wide involvement in many processes, the phenotypic and physiological effects of N-terminal acetylation are highly varied, seemingly dependent on multiple variables, including the protein affected, the NAT complex responsible for acetylation, and the organism in which the process occurs. As mentioned previously, reduced N-terminal acetylation due to knockout of certain NAT complexes lead to fragile growth phenotypes but general viability in yeast. Such a result suggests that N-terminal acetylation is important to maintaining function in only some proteins; however, the consequence of organismal complexity must be considered.

Notably, disturbances in N-terminal acetylation often resulting in the onset of potentially lethal diseases in humans. For example, N-terminal acetylation has a suggested role in the onset of neurodegenerative disease. α- synuclein is a primarily neuronal protein that is known to assemble into amyloid fibrils, the onset of which characterizes the often-lethal Parkinson's disease (PD) and dementia with Lewy Bodies (DLB) (Kang et al. 2012; Anderson et al. 2006). N-terminal acetylation is known to affect the secondary structure of α-synuclein in important functional regions, likely attributable the stabilization of helicity by neutralization of charge. N-terminal

acetylation of α-synuclein generally results in both short and long-range conformational effects accompanied by altered rates of fibril assembly (Kang et al. 2012).

Ogden's syndrome, the first human genetic disorder directly linked to a mutation in NatA, provides another striking example of N-terminal acetylation in human disease (Van Damme et al. 2014). Ogden's syndrome is an X-linked disorder that manifests symptomatically by the appearance of cranial abnormalities, hypotonia, and cardiac issues, eventually culminating in infant mortality (Van Damme et al. 2014). NATs have also been implicated as both potential oncoproteins and tumor suppressors, with NAT expression being varied in cancerous and non-cancerous tissues (Kalvik et al. 2013). Furthermore, manipulated NAT expression in cancer cells resulted in apoptosis, autophagy or even cell-cycle arrest (Kalvik et al. 2013).

The purpose of N-terminal acetylation in cells continues to be enigmatic due to the variety of effects resultant of this modification. However, its evolutionary importance is clear due to its appearance prevalence in eukaryotes. Move over, due to its known regulatory roles in cellular processes and implied roles in disease, it is of great importance to continue to define the downstream N-terminal acetylation as it may improve scientific understanding in these areas.

Purification of Hsp70

A majority of studies focused on Hsp70s use *S. cerevisiae* as an expression system due to its similarity to higher eukaryotes in protein processing and modification (Needham et al. 2015). Among the fourteen Hsp70 homologs expressed in yeast, the cytoplasmic Ssa (Stress seventy A) proteins, comprised of Ssa1-4, are the most well-

studied (Needham et al. 2015; Shaner et al. 2005). The Ssa subfamily is the only cytosolic subfamily of Hsp70s that is essential (Needham et al. 2015; Shaner et al. 2005; Wegele et al. 2003b). While all Ssa proteins are expressed differentially, at least one of the possible four Ssas must be expressed for cell viability (Shaner et al. 2005; Wegele et al. 2003b). Of the other Ssa chaperones, Ssa1 is of particular interest due to its dynamic gene expression under varied physiological conditions and its roles in proteostasis and prion propagation (Needham et al. 2015; Shaner et al. 2005; Wegele et al. 2003b).

Current studies of Ssa1 prove limited due to the capacities and intentions of current purification methods. While several methods exist, they are fairly similar in approach, and are often both resource intensive and time-consuming. To demonstrate this point, the details common to Ssa1 purification methods that are used within the field will be briefly summarized.

The majority of Ssa1 purifications require a high initial cell density prior to lysis, as most protocols require cell density measurements to approximate 10 ODs to achieve sufficient chaperone yield (Cyr et al. 1992, Needham et al.2003). One method calls for a starting OD of 2.5, though in this method, Ssa1 is expressed in *Pichia pastoris* rather than its endogenous yeast. *P. pastoris* is a notable eukaryotic expression system because it can achieve gram amounts of recombinant protein per liter of culture by secretory and intracellular means (Ahmad et al.2014; Wegele et al. 2003.) Noting this exception, 2-6 liters of starting cell culture is typical for methods using *S. cerevisiae*, emphasizing the need for high starting cell densities to obtain a reasonable yield (Cyr et al. 1992).

Often cells are lysed via glass bead lysis (Cyr et al. 1992; Needham et al. 2003; Wengele et al. 2003), followed and several rounds chromatography. A combination of

affinity chromatography and ion-exchange chromatography is commonly used to obtain Ssa1 fractions from cell lysates (Cyr et al. 1992; Needham et al. 2003). By utilizing both ion-exchange column chromatography, which separates ionizable molecules based on their total charge (GE Healthcare, 2018), and affinity chromatography, a technique which utilizes the specific interaction between an immobilized ligand and the protein of interest to isolate the desired protein from its surrounding mixture (GE Healthcare, 2016), it is relatively ensured that pure Ssa1 protein will be isolated.

If not immediately precipitated (Wengele et al. 2003), chaperone fractions are combined, dialyzed, concentrated, and subjected additional rounds of chromatography in order to ensure purity of the sample (Cyr et al. 1992; Needham et al. 2003; Wengele et al. 2003). Some methods will alternate different chromatographic approaches to enhance purity and yield, as exemplified by one method which used hydrophobic interaction chromatography, a technique that separates based on hydrophobicity (GE Healthcare, 2018) followed by size exclusion chromatography, which separates molecules based on molecular size (GE Healthcare, 2018c; Wengele et al. 2003).

Protein purity was seldom reported, though one method stated that Ssa1 preparations were 98% pure (Cyr et al. 1992). Chaperone yields reported varied between methods, though several yields were within the milligram range, indicating reasonable purification efficiency (Needham et al. 2003; Wengele et al. 2003). Notably, only one method utilized an affinity tag, namely a His tag, to purify Ssa1 by affinity chromatography (Aron et al. 2005). While this method was efficient and obtained a reasonable yield, its use of an affinity-tag emphasized its novelty when compared to other purification schemes for Ssa1.

From parsing protocols used in the field, it is clear that Ssa1 purifications are generally demanding in terms of resources, time, and experience. Most methods are large-scale, multistep, and produce similar chaperone yields and purity. Whiles such methods suit their general purpose, they are generally exclusionary to smaller institutions that lack the necessary resources.

Realizing this opportunity, we developed a highly efficient, one-step purification method that is both user-friendly and affordable. By using a Ssa1-Protein-A fusion strain in combination with IgG-conjugated magnetic beads, our method facilitates purification by the high-affinity interaction between the Protein-A tagged Ssa1 and IgG-conjugated magnetic beads. Using this purification method, we avoid using expensive of chromatography columns in lieu of magnetic Dynabeads, which are more affordable, and can be conjugated to IgG in house. We have eliminated the need for large starting culture volumes as this method obtains high yields of Ssa1 from a starting OD of 5, which can typically be achieved by 25mL cultures. Notably, the yields that are achieved by this purification are in a 3-fold increase compared to those reported by similar methods (Griffith et al. 2018). Furthermore, our method is compatible with native elution, yielding enzymatically active chaperone (Griffith et al. 2018), allowing for the future study of Ssa1 in the context of N-terminal acetylation.

Materials and Methods

Cell culture

Yeast were grown in standard rich media YPD in either a roller drum or shaking incubator at 30°C and harvested at mid-to late-exponential phase as determined by optical density (OD_{600}). *E. coli* were grown in standard LB in either a roller drum or shaking incubator at 37°C and harvested when $OD_{600} \geq 0.5$.

SDS-PAGE and Western blotting

Samples were resolved on a polyacrylamide gel and stained with Coomassie BB R-250 (Thermo Fisher) or transferred to a PVDF membrane for Western blot analysis. Anti-Ssa1/2 (Invitrogen), anti-Gpd1 (Thermo Fisher), anti-GAPDH (Thermo Fisher), and anti-Ydj1 (Thermo Fisher) were used to probe resolved proteins, with Goat-anti-rabbit HRP (Thermo Fisher) used as a secondary antibody. Proteins were visualized by ECL (Thermo Scientific) and imaged using a ChemiDoc XRS+ imaging system (Bio-Rad).

Ssa1-PrA Purification

Cultures were grown in YPD liquid media and were continually diluted to maintain exponential phase growth for 24 hours before lysis. 15 OD of exponentially growing culture were pelleted and washed with cold distilled water. Cells were pelleted in a 2.0mL flat bottom microcentrifuge tube at 13,000 rpm for 5 minutes at 4°C. Cells were then resuspended in cold lysis buffer (20mM Tris-HCl (pH 8.0), 150mM NaCl, 10mM $MgCl_2$, 2mM PMSF, protease inhibitor tablet (Thermo Fisher Scientific), and 1mM EDTA). Glass beads were then added to a total volume of 1mL and vortexed for 7

minutes at 4°C. Cell lysates were separated from glass beads and mixed with 10x detergent (20mM Tris-HCl (pH 8.0), 150mM NaCl, 10mM MgCl2, 1% NP-40, and 0.25% Na-deoxycholate).

500µL of lysate-detergent mix was introduced to 50µL of IgG conjugated magnetic Dynabeads and allowed to nutate at 4°C for at least 1.5 hours. The supernatant was removed, and magnetic beads were washed once in wash buffer (20mM Tris (pH 8.0), 150mM NaCl, 10mM $MgCl_2$, 1% NP-40, 0.25% Na-deoxycholate) at 4°C and three times at room temperature. Magnetic beads were washed once with 1mL of 50mM Tris-HCl (pH 7.0) at room temperature. Proteins were prepared for SDS-PAGE by either heating for 10 minutes at 70°C in non-reducing SDS buffer (150mM Tris-HCl pH 6.8, 30% glycerol, 6% SDS, 0.03% bromophenol blue) to detect any non-covalently associated proteins or boiled for 3 minutes in SDS-PAGE sample buffer for total protein detection.

Native Elution of Ssa1

Ssa1 was eluted under native conditions by incubating washed magnetic beads with 30µL of elution buffer (0.1M sodium acetate pH 3.5), followed by immediate neutralization by the addition of 3µL of 1.5M Tris (pH 8.8). Native Ssa1 elution was achieved by incubating washed magnetic beads with a 1:300 dilution of PreScission Protease (PPX, GE Healthcare) for 16 hours at 10°C.

Proteinase K digestion

Eluted Ssa1 protein was concentrated using a Micron YM-30 centrifugal filter and reservoir (Millipore) at 14000 x g for 14 minutes at 4°C. A buffer exchange was performed the concentrated protein by adding 25µL of cold Proteinase K assay buffer (25mM Tris pH 7.4, 50mM KCl, 5mM $MgCl_2$) and repeating centrifugation under the previous specifications. The concentrated protein was resuspended in 22.4µL of Proteinase K assay buffer and transferred into a new reservoir. 2.5µL of 50mM ATP was then added and the mixture remained at room temperature for 20 minutes. An 8µL sample was taken before addition of the Proteinase K as a negative control. 1µL of 1:100 Proteinase K was added to the mixture. 8µL samples were taken at 5 and 15 minutes, respectively. All samples were introduced to an equal volume of 40% T.C.A. and remained at 4°C for 30 minutes after completion of the digestion reaction. Samples were centrifuged at 13.3 x 10^3 min^{-1} at 2°C for 20 minutes. Pelleted protein was then washed with 500µL of cold 100% acetone and resuspended in SDS-PAGE sample buffer.

Isoelectric Focusing of Ssa1-PrA

55µL of 10x detergent was added yeast cell lysates. Lysates were then mixed with IEF sample buffer (Bio-Rad) in a 1:5 proportion and remained on ice until gel loading. Lysates were resolved on a Criterion IEF Pre-Cast gel pH 3-10 (Bio-Rad) on a Criterion cell (Bio-Rad) as per manufacturer's instructions. The IEF gel was protonated in 0.1% acetic acid mixture for 5 minutes, followed by submersion in distilled water for 1 minute. Resolved proteins were transferred to a PVDF membrane using a Trans-Blot Turbo Blotting System (Bio-Rad) and were probed by Western blot.

Cross-linking of Ssa1 and associated proteins

Duplicate cultures were grown in YPD liquid media and were continually diluted to maintain exponential phase growth for 24h before lysis. 15 OD equivalents were pelleted and washed twice with reaction buffer (1M HEPES pH 7.5) before resuspension in reaction buffer. 75µL crosslinker solution (20mM DSP (Thermo Fisher) in dry DSMO) was added to reach a final concentration of 1.5mM of the crosslinker solution. The reaction mixture remained at room temperature for 30 minutes. Stop solution (1M Tris pH 7.5) was then added to the reaction mixture to a final concentration of 15mM, remaining at room temperature for 15 minutes. After 15 minutes, cells were pelleted and washed three times with cold lysis buffer. Cells were lysed by glass bead lysis and Ssa1-PrA and any associated proteins were co-purified from cell lysates as previously specified.

Transformation of Ydj1 plasmid

1µL of purified Ydj1 plasmid was added to 50µL of DE3 competent cells and the mixture sat on ice for 30 minutes. Cells were heat-shocked for 3 minutes at 37°C and immediately transferred back to ice. Cells remained on ice for at least 2 minutes, after which, 250µL of LB was added to the cells and allowed to grow in a roller drum at 37°C for 20 minutes. 75µL of transformed cells were then plated onto a solid LB +amp plate and sat for 1 minute at room temperature before the plates were inverted and incubated for 12 hours at 37°C.

Purification of Ydj1

Transformed cells were grown in LB+amp liquid media and continually diluted to maintain exponential phase growth for 24 hours. Before lysis, cells were transferred to 500mL of fresh LB+amp followed by induction with IPTG for 3 hours under standard growth conditions. Induced cells were pelleted, resuspended in 50mL lysis buffer (50mM Tris pH 9.0, 50mM NaCl, 1 protease tablet; 50μM PMSF), and lysed by sonication. Cell lysates were pelleted at 15000 RPM for 30 minutes at 4°C. Ydj1 was purified using a 5mL HisTrapFF nickel Sepharose affinity column on a fast protein liquid chromatography (FPLC) ÄKTA system, both obtained from GE Lifesciences. The column was initially washed before sample injection with Buffer A (50mM Tris pH 9.0; 150mM NaCl) (flow rate: 3.0mL/min). 41mL of cell lysates were then loaded onto the column (flow rate: 2.0mL/min). Column bound proteins were washed with 10 column volumes of Buffer A and followed by elution with 4 column volumes of Buffer B (50mM Tris pH 9.0; 150mM NaCl; 250mM imidazole). 1mL fractions were collected manually during each phase of the purification with the exception of the elution, wherein a 5mL fraction was collected during the corresponding mAU peak that indicated the elution of column bound Ydj1. All chromatographic data and the execution of the purification protocol was administered and recorded by Unicorn start software version 1.1. 15μL samples were obtained from the respective collected fractions and were then mixed with SDS-PAGE sample buffer.

Results

To understand the effects of N-terminal acetylation on Ssa1 chaperone function, we needed to develop a specific pull-down protocol of Ssa1 without disrupting any modification of the N-terminus. To accomplish this goal, a Ssa1-PrA fusion construct was transformed into both wild-type (WT) and N-terminal acetylation-deficient backgrounds, (Δard1 and S2P, respectively). The Ssa1-PrA fusion construct features a Protein-A affinity tag at the extreme C-terminus of Ssa1. Because of the naturally occurring affinity between IgG and Protein A, the Protein-A tag allows for pull-down of the tagged chaperone when used in combination with magnetic Dynabeads conjugated with rabbit IgG. The Ssa-PrA fusion construct additionally encodes a precision protease cut site located upstream of the C-terminal affinity tag, allowing for specific proteolytic cleavage of the affinity tag from the chaperone when desired.

WT Ssa1 is known to be N-terminally acetylated, though is expected that the chaperone will not be N-terminally acetylated by the NatA when expressed in either the Δard1 or S2P backgrounds. In Δard1 background, the NatA complex lacks its catalytic subunit, blocking the N-terminal acetylation for all targets of NatA, including Ssa1. In the S2P strain, the serine residue at the second position of Ssa1 within the N-terminus is changed to proline, specifically blocks N-terminal acetylation of Ssa1 via the XPX rule. Expression of the Ssa1-PrA fusion construct in these three genetic backgrounds respectively allows for comparison-based chaperone activity studies in the context of N-terminal acetylation.

The expression of our fusion protein in WT and N-terminal acetylation-deficient genetic backgrounds was previously confirmed. To quantify Ssa1-PrA expression, the

total protein content of cell lysates was resolved by SDS-PAGE. Cell lysates were probed with an Hsp70-specific antibody to ensure the specificity of the Protein-A fusion, while a GAPDH-specific antibody established the load control. Because Protein-A is bound specifically by antibodies containing an IgG-heavy chain, Protein-A is recognized by goat anti-rabbit HRP, allowing for visualization of the Ssa1-PrA fusion protein; therefore, both Ssa1 and Protein-A were visualized by immunoblot (Figure 1). Ssa1-PrA was expressed consistently in all three of the evaluated genetic backgrounds. Parent-strains produced a single band by Western blot, while transformed strains produced two bands. The band present at the higher molecular weight represents the Ssa1-PrA fusion protein, which has a higher molecular weight than endogenous Ssa1 due to its Protein-A affinity tag; while the band present at the lower molecular weight is endogenously expressed Ssa2.

After confirming expression, we next developed a protocol that would purify Ssa1-PrA from WT cell lysates. Therefore, we adapted a purification method that used magnetic Dynabeads conjugated with rabbit IgG to facilitate Ssa1-PrA pull-down the naturally high-affinity interaction between Protein-A and IgG. Ssa1-PrA pull-down was highly specific, as non-specific proteins were not observed with colloidal Coomassie Blue stain (Figure 2). A single band of approximately 55-kDa was observed, though this band is the heavy chain of the rabbit IgG and is expected under the denaturing conditions of the SDS-load buffer (Figure 2, lanes 5 and 6). Silver stain confirmed the specificity of Ssa1-PrA pull-down as non-specific proteins were not observed (Figure 3). Immunoprecipitants from WT, Δard1, and S2P strains resolved by gel electrophoresis indicated that Ssa1-PrA pull-down was consistent for all generated strains (Figure 4).

While Ssa1-PrA immunoprecipitants were highly pure, we next wanted to assess the quantity of chaperone that was obtained via our pull-down method. Ssa1-PrA immunoprecipitants obtained from a 5 OD equivalent of WT cells were resolved by SDS-PAGE alongside a BSA titration, ranging from 10 to 25µg (Figure 5). The band intensity corresponding to the immunoprecipitated Ssa1-PrA was intermediate to that of the 10 and 25µg BSA, suggesting that approximately 15µg of Ssa1-PrA can be obtained from 5mL of exponentially growing culture as starting material.

Though Ssa1-PrA pull-down was both highly specific and efficient, the Ssa1 chaperone network is diverse and subject to interaction of Ssa1 with a wide variety of co-chaperones, nucleotide-exchange factors, and client proteins; all of which modulate chaperone activity. In addition to these factors, both x-ray crystallographic analyses (Wilbanks and McKay, 1995) and kinetic assays (Feifel et al. 1999) indicated that monovalent ion identity dramatically influences enzymatic activity by stabilizing the N-terminal nucleotide binding cleft. From these studies, it was determined K^+ promoted maximal ATPase activity and client binding, while Na^+ induced minimal levels of these activities (Feifel et al. 1999); therefore, we next assessed if our method could co-purify Ssa1 in complex with one of clients by repeating Ssa1-PrA pull-down under low and high salt concentrations (150mM and 300mM, respectively) and with NaCl substituted for KCl. While we did not observe confirmed pull-down of Ssa1 clients, different amounts of Ssa1-PrA were pulled-down under each condition (Figure 6), demonstrating that pull-down is robust under altered experimental conditions. These data suggest that our method may have an alternative use in the quick optimization of pull-down conditions necessary for downstream analyses.

Though pull-down was highly specific, efficient, and robust, the removal of Ssa1-PrA from magnetic beads was achieved under denaturing conditions. Denaturing conditions inactivate the chaperone, rendering it unsuitable for downstream analyses requiring enzymatic activity. The dissociation of IgG bound to Protein-A Sepharose columns can be achieved using an elution buffer with a pH of 3.5 (Duhamel et al. 1979); therefore, we repeated the immunoprecipitation of Ssa1-PrA to determine whether a similar pH shift could elute our fusion protein from our magnetic beads sufficiently. Proteins were eluted with 0.1M sodium acetate buffer (pH 3.5) followed by subsequent neutralization of eluates with 1.5M Tris buffer (pH 8.8). Ssa1-PrA was found to elute under these conditions, though a portion of the fusion protein remained associated with the beads post-elution (Figure 7). Nevertheless, using the pH shift acted sufficiently as a native elution technique for Ssa1-PrA, preserving both native chaperone structure and ensuring compatibility with downstream assays.

Using the pH shift as a native elution technique allowed for timely elution of Ssa1-PrA from the IgG-conjugated magnetic Dynabeads, though it did not address the C-terminal Protein-A affinity tag, the presence of which may inherently hinder structural characterization of natively isolated chaperone. The Ssa1-PrA construct was designed to include a PreScission protease (PPX) cut-site upstream of the C-terminal Protein-A affinity tag. PreScission protease is highly specific, cleaving between Gln and Gly residues of its recognition sequence LeuGluValLeuPheGln/GlyPro, resulting in a reduced likelihood of off-target proteolysis. Digestion of Ssa1-PrA by PreScission protease results in the removal of the Protein-A tag and the native elution of Ssa1 (Figure 8a). Ssa1

elution appears to be complete with no uncut fusion protein associated with the magnetic beads, as only IgG and Protein-A are visible by colloidal Coomassie stain (Figure 8b).

Eluting Ssa1-PrA by PreScission protease yielded highly pure Ssa1 chaperone under native conditions. Presumably, removal of the Protein-A affinity tag yields chaperone that was structurally comparable to endogenously expressed Ssa1. It was reported that partial proteinase K digestion of Ssa1 in the presence of ATP produces a distinct 45-kDa fragment, indicative of N-terminal nucleotide-binding domain (NBD), as well as a transient fragment of approximately 60-kDa, representing the protected C-terminal substrate-binding domain (SBD) in the ATP-bound state (Needham and Masison 2008). To determine whether characteristic features of Ssa1 structure could be observed, we attempted a partial Proteinase K digestion of our eluted Ssa1 protein (Figure 9). Before the introduction of Proteinase K, two distinct bands were observed at 75- and 45-kDa, indicative of our undigested chaperone and the N-terminal NBD, respectively. A third band was also observed at 60-kDa, which is consistent with the C-terminal SBD. At five minutes after the introduction of the Proteinase K, the 75-kDa band was no longer visible. Furthermore, the 60-kDa band becomes highly faint by this time-point. The 60-kDa band completely disappears by fifteen minutes, leaving only the 45-kDa band present by the end of the observation period. These data suggest that eluted Ssa1 is structurally comparable to endogenous chaperone.

While it is predicted that N-terminal acetylation is necessary for proper Ssa1 function, both non-N-terminally acetylated and N-terminally acetylated chaperone are required to fully elucidate the effect of this modification on chaperone activity via comparative analyses. We next focused on confirming the expected N-terminal

acetylation status of Ssa1 in our established genetic backgrounds by isoelectric focusing (IEF). IEF is an electrophoretic procedure wherein zwitterionic molecules are separated by isoelectric point (pI), the pH wherein the net charge of the resolved molecule is zero (Brasher and Thorpe, 1998). pI values are known to change when target proteins are modified, resulting in a discernable change in protein migration between the modified and unmodified forms. There is a visible migratory shift between WT Ssa1-PrA and Δard1 Ssa1-PrA when resolved by IEF and probed by Western blot with Ssa1/2 specific antibody. The band for WT Ssa1-PrA runs more acidic than Δard1 Ssa1-PrA, indicating the N-terminal acetylation of WT Ssa1-PrA and the absence of this modification in the Δard1 background (Figure 10).

There are various mechanisms by which N-terminal acetylation may alter Ssa1 activity; however, altering the association of Hsp70 co-chaperones is a likely mechanism which would stand to affect several downstream processes due to the expansiveness of the Hsp70 chaperone system. By reconstituting components of the Hsp70 chaperone system *in vitro*, it is possible to use a comparative approach to assess whether N-terminal acetylation alters co-chaperone binding, and therefore, Ssa1 activity. We began our effort to reconstitute the Hsp70 chaperone system by attempting to co-purify Ssa1-PrA with endogenous Hsp40, a major co-chaperone family to Hsp70. To co-purify Hsp40, we intracellularly crosslinked Ssa1-PrA with endogenous co-chaperone with DSP prior to purification. Coomassie stain revealed that Ssa1-PrA failed to facilitate pull-down of endogenous Hsp40 or other co-chaperones involved in the Hsp70 chaperone system (Figure 11).

The inability to co-purify endogenous co-chaperones by crosslinking suggests that the purification of Hsp40 would likely have to occur separately from that of Ssa1 to allow for future studies requiring the co-chaperone to evaluate in Ssa1 activity in the context of N-terminal acetylation. We first expressed an Hsp40 co-chaperone of Hsp70, Ydj1, in competent *E. Coli* DE3 cells. While the Hsp40 is endogenously expressed in *S. cerevisiae*, expressing Ydj1 in a prokaryotic system blocks post-translational modification, preventing downstream changes in Ssa1 activity that may be attributable to the modification of Ydj1 rather than changes in Hsp70 N-terminal acetylation. DE3 cells were transformed with an expression plasmid containing His-tagged Ydj1 under an IPTG-inducible promoter. Cell lysates from uninduced cultures and those induced with IPTG were resolved by SDS-PAGE and probed by Western blot using Ydj1-specific antibody, which revealed that induced cells expressed His-tagged Ydj1 (Figure 12).

Once the expression of His-tagged Ydj1 was confirmed, we then purified Ydj1 for use in binding assays. Using immobilized metal affinity chromatography (IMAC), it is possible to use the affinity between the histidine tag and the nickel Sepharose immobilized within a fast protein liquid chromatography (FPLC) HisTrapFF column (GE Lifesciences) to isolate our protein of interest from cell lysates. Protein concentration is measured by absorbance at 205nm as a function of flow through the nickel Sepharose column, producing the chromatograph in Figure 13a. The total protein content of the cell lysates (FT: 0-45mL) were run through the column, washed, and the elution of His-tagged Ydj1 from the column is indicated by the peak in mAU absorbance at 100mL. When proteins from purification fractions were resolved by SDS-PAGE, pull-down of

His-tagged Ydj1 appears to be relatively specific as few contaminating bands were present within the elution fraction, as indicated by Coomassie Blue stain (Figure 13b).

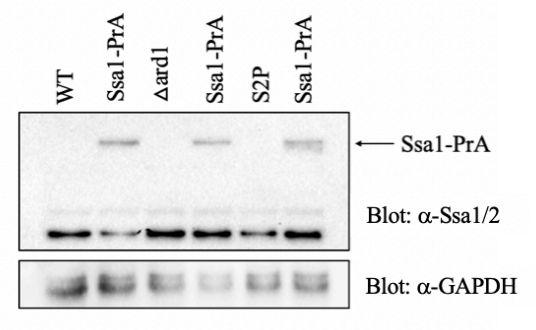

Figure 1. **Protein-A fusion Ssa1 chaperone (Ssa1-PrA) is expressed in both WT and N-terminal acetylation deficient backgrounds, allowing for purification and future comparative analyses.** Lysates from wild-type (WT) and N-terminal acetylation deficient (Δard1, S2P) backgrounds were resolved by SDS-PAGE, transferred to PVDF membrane, and probed for Ssa1/2. Membrane was re-probed for GAPDH as a load control.

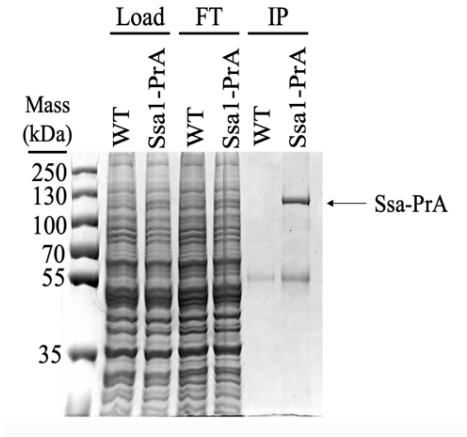

Figure 2. **IgG-conjugated magnetic beads facilitate pull-down of Ssa1-PrA from cell lysates. (FT)** Lysates nutated end-over-end with IgG-conjugated magnetic Dynabeads for 1.5 hours at 4°C. **(IP)** Beads were boiled with SDS. Proteins were separated by SDS-PAGE and stained with Coomassie Blue dye.

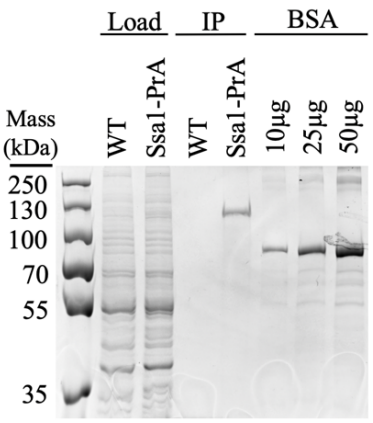

Figure 4. **Quantification of purified Protein A-tagged Ssa1 by BSA titration indicates that method is highly efficient, yielding 15 ug per 5 OD equivalent.** (IP) Beads were heated in LDS to interrupt non-covalent interactions. Proteins non-covalently associated with beads were boiled in SDS. Proteins were separated by SDS-PAGE and stained with Coomassie Blue dye. *confirmed by Bradford assay (data not shown)

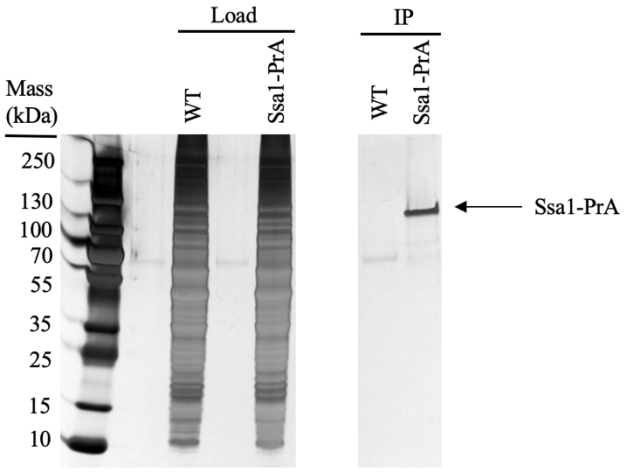

Figure 3. **Silver stain of Ssa1-PrA pull-down indicates that method is highly specific and yields pure chaperone. (IP)** Beads were boiled with SDS. Proteins were separated by SDS-PAGE and stained with Silver Stain (Pierce) per manufacturer's instructions.

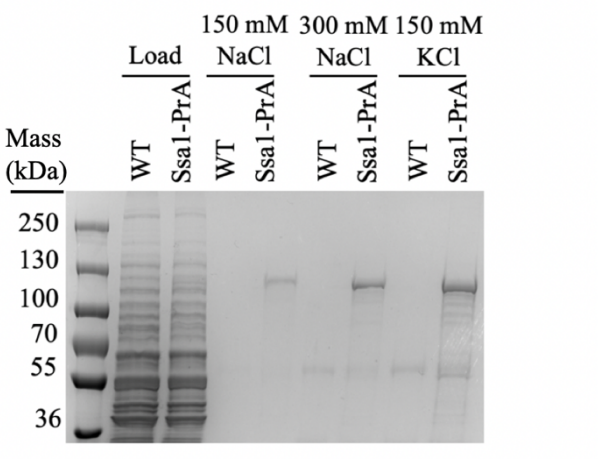

Figure 5. **Ssa1-PrA pull-down is unaffected by altered ionic conditions, indicating that method is robust and may prove useful in prototyping experimental conditions**. To investigate claims on the differential effects of Na^+ and K^+ on the stability of Hsp70-polypeptide complexes, Ssa1-PrA pulled -down under different ionic conditions. Salt type and concentration are shown. Beads were boiled with SDS. Proteins were separated by SDS-PAGE and stained with Coomassie Blue dye.

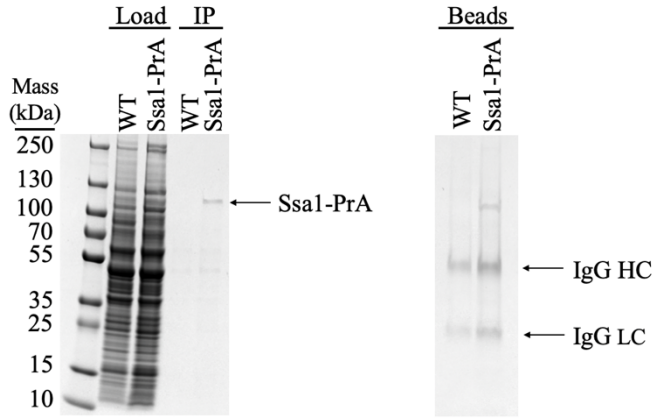

Figure 6. **Purification method is compatible with pH shift, facilitating elution of Ssa1-PrA under native conditions.** IgG-conjugated magnetic Dynabeads with non-covalently linked Ssa1 were incubated in 0.1M sodium acetate pH 3.5 at 35°C for 16 minutes. Eluates were neutralized using 1.5M Tris pH 8.8. Post-elution beads are shown. Arrows indicate remaining IgG heavy chain **(HC)**, light chain **(LC).** Proteins were separated by SDS-PAGE and stained with Coomassie Blue dye.

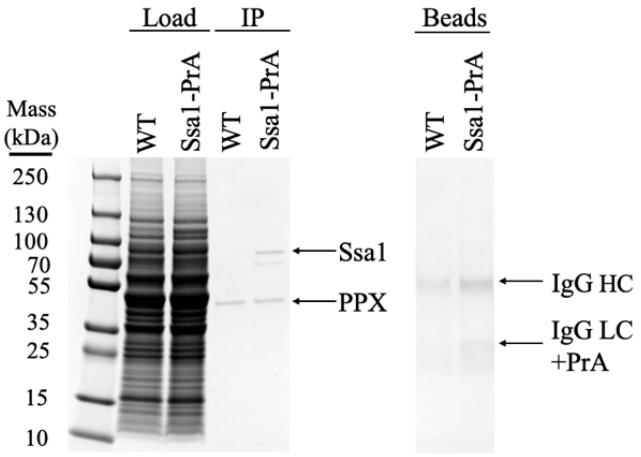

Figure 7. **PrA tag is cleaved from Ssa1 via Pre-Scission protease (PPX) providing a second native elution technique that addresses C-terminal PrA tag.** The native elution of Ssa1 was achieved by using 1:300 dilution of Pre-Scission protease (GE Healthcare) at 10°C for ≥16 hours. Post-elution beads are shown. Arrows indicate remaining IgG heavy chain **(HC)**, light chain **(LC)**, or Protein-A **(PrA)**. Proteins were separated by SDS-PAGE and stained with Coomassie Blue dye.

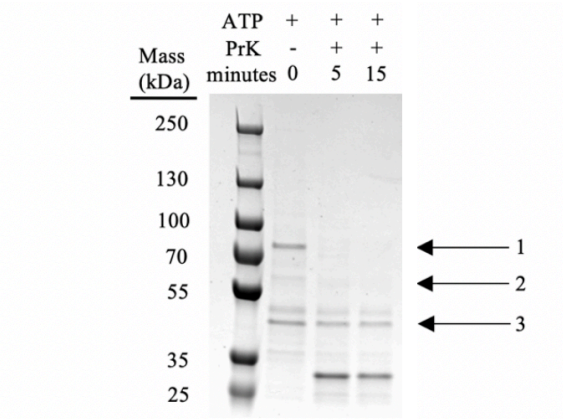

Figure 8. **Partial-digestion of PPX-eluted Ssa1 by Proteinase K indicates characteristic Ssa1 structure.** Ssa1 protein was incubated at 25°C with 5 mM ATP for 20 minutes, and then digested by proteinase K **(PrK)** for 5 or 15 minutes at 25°C. Proteins were separated by SDS-PAGE and stained with Coomassie Blue dye. Arrows indicate the positions of reaction products previously characteristic to Ssa1 digestion.

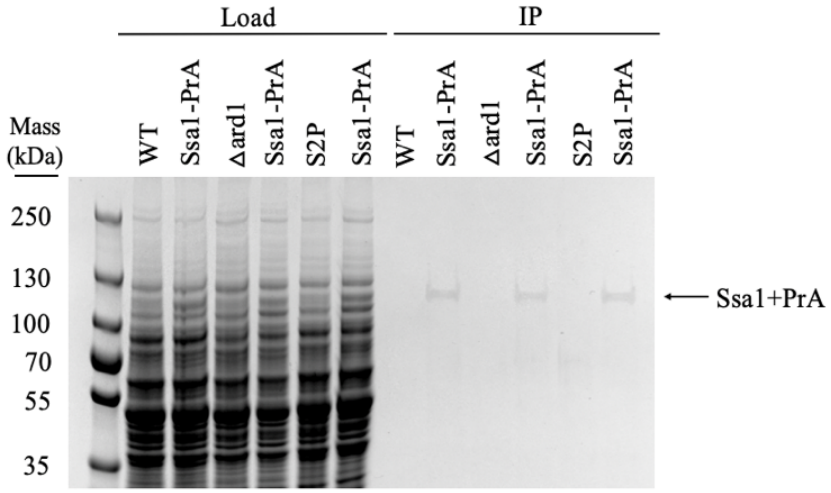

Figure 9. **Ssa1-PrA pull-down is consistent across both WT and N-terminal acetylation deficient strains (Δard1, S2P), allowing for future comparative analyses. (IP)** IgG-conjugated magnetic Dynabeads were heated in LDS, interrupting non-covalent interactions. Non-covalently associated proteins were boiled in SDS load buffer. Proteins were separated by SDS-PAGE and stained with Coomassie Blue dye.

Figure 10. I**soelectric focusing of Ssa1-PrA from WT and ∆ard1 knockout indicates that Ssa1 is N-terminally acetylated by the NatA complex.** Cell lysates from both WT and ∆ard1 yeast strains expressing Ssa1-PrA were resolved by isoelectric focusing on a Criterion IEF Pre-cast gel pH 3-10 (Bio-Rad) per manufacturer's instructions. Gel was protonated in 0.7% acetic acid for 5 minutes and transferred to PVDF membrane. Membrane was probed by for GPD1.

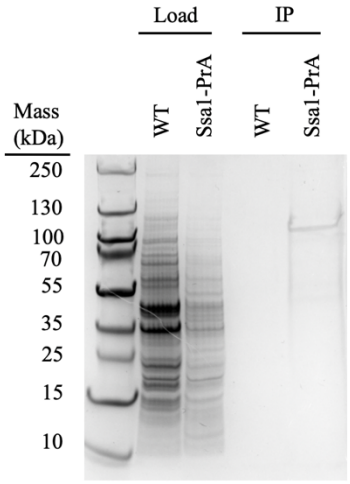

Figure 11. **Failure of Ssa1-PrA to crosslink with endogenous Hsp40 suggests that purification of exogenous Hsp40 is necessary to conduct future Hsp70 characterizations.** Intracellular Ssa1-PrA was crosslinked to associated binding partners prior to IP using DSP. Lysates nutated end-over-end with IgG-conjugated magnetic Dynabeads for 1.5 hours at 4°C. **(IP)** Beads were boiled with standard SDS load buffer. Visualized by SDS-PAGE/Coomassie stain.

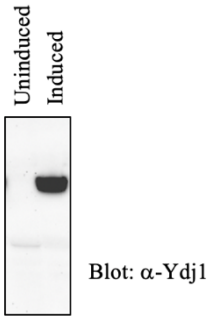

Figure 12. **Ydj1 is expressed in transformed DE3 cells upon induction with IPTG**. Lysates from uninduced and induced DE3 cells transformed with Ydj1 plasmid were resolved by SDS-PAGE, transferred to PVDF membrane, and probed for Ydj1.

A.

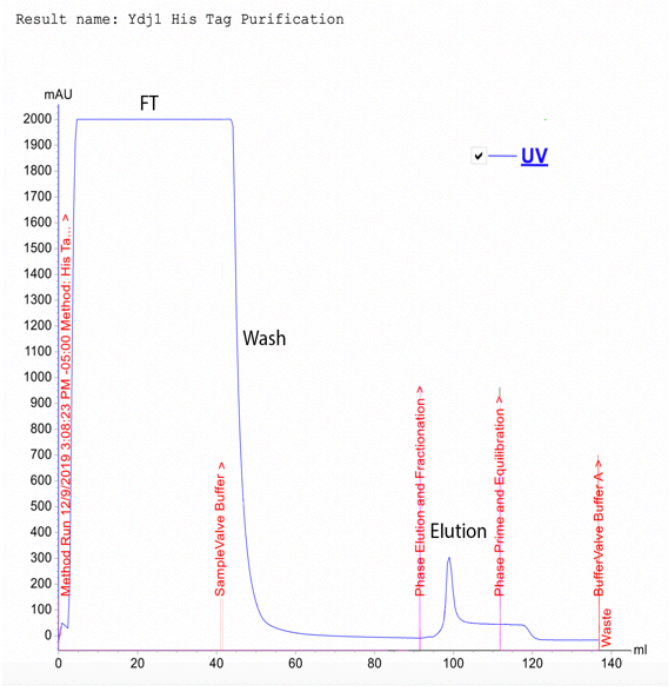

B.

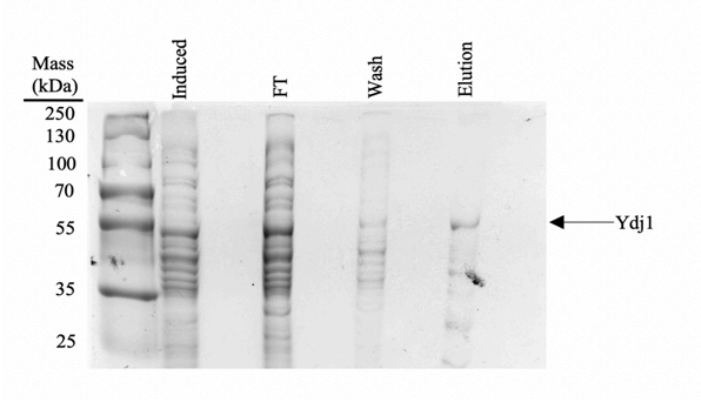

Figure 13. **His-tagged Ydj1 is pulled-down via IMAC.** A. (Induced) Cell lysates of induced DE3 cells prior to loading onto the HisTrapFF column. (FT) After column loading, proteins that did not bind to column were collected. (Wash) Proteins that dissociated from column upon wash stage of purification were collected. (Elution) Column-bound proteins separated from column. Sample fractions were separated by SDS-PAGE and stained with Coomassie Blue. B. Chromatograph corresponding to Ydj1 purification. Total volume processed by the column during purification is indicated at the X-axis. Absorption of mAU values (indicating protein detection at 205 nm) recorded during the course of purification is shown at the Y-axis. Stages of purification are marked.

Discussion

In this study, we developed a one-step purification of Ssa1 from *S. cerevisiae* through the collective integration of several purification techniques. This method utilizes the high affinity interaction that occurs between Protein-A and IgG to facilitate a highly specific pull-down of Ssa1, as indicated by Coomassie Blue stained (Figure 2) and Silver-stained SDS-PAGE (Figure 3). The use of IgG-conjugated magnetic Dynabeads enhances purification efficiency as the beads remain mobile in solution, allowing for maximum contact with soluble protein while also exhibiting a low rate of non-specific binding. While the IgG can be stripped from the beads during elution, it is possible to re-conjugate IgG to the beads after use, minimizing unnecessary cost. Elution by pH shift should not affect the conjugation of the IgG to the beads and if elution is accomplished using PreScission protease, the interaction between the Protein-A and IgG can be interrupted by pH shift and the IgG-conjugated beads can be separated from the Protein-A tag. Additional cost is also avoided as this method is able to purify a significant amount of Ssa1 from a limited amount of starting material, as 3.0μg of chaperone is obtained per mL of exponentially growing culture, which stands as a significant improvement to yields obtained by similar methods (Griffith et al. 2018). In all cases, material cost is reduced.

Is it notable that this method yields highly pure chaperone in one-step, considering that most proteins require a series of steps to be purified (Labrou N., 2014). The ability to purify in one-step is highly desirable in protein purification, as it negates costs associated with subsequent purification steps, additional materials and technologies, and maximizes time-efficiency. The degree of chaperone purity is maintained under native elution conditions (Figure 6, Figure 7), and while an additional step is required to

remove the PreScission protease, it is performed with common reagents due to the PreScission protease containing a GST-affinity tag. It should be noted that removal of the PreScission protease from purified Ssa1 is unnecessary except in very specific cases due to the highly specific action of the enzyme.

All data suggests that the Ssa1 obtained this method is representative of its endogenous condition, as elution by PreScission protease cleavage did not affect the structural integrity of the chaperone, evidenced Proteinase K digestion (Figure 8). A potential concern arises in the placement of the Protein-A tag at the extreme C-terminus of the chaperone, as this region facilitates interactions with Hsp70 co-chaperones and substrates via the C-terminal SBD (Gong et al. 2018). Additionally, the combined effects of the location and relative size of the Protein-A tag may impede client and co-chaperone interactions, which may explain the failure of our cross-linking attempt (Figure 11). However, due to the presence of functionally redundant isoforms of Ssa within the cytosol, it is unlikely that such an inability of Ssa1-PrA to engage in typical chaperone interactions would pose any detriment to cell viability.

Arguably, the positioning of the Protein-A tag at the C-terminus is non-negotiable, as it preserves the structural integrity of the N-terminus and permit its modification, as emphasized by the determination that WT Ssa1-PrA is N-terminally acetylated by IEF (Figure 10). A potential solution may be to express a new construct that extends the linker sequence which connects the extreme C-terminus and the Protein-A tag, thereby removing any steric hindrance that is associated with the Protein-A tag, allowing for normal chaperone interaction to occur. However, the retained ATPase activity of WT Ssa1-PrA after cleavage of its Protein-A tag suggests that the tag does not

permanently impair chaperone function (Griffith and Holmes, 2018). While the presence of the tag may impede the co-purification of Ssa1-associated proteins, the effect of the tag on chaperone activity or binding should be negligible *in vitro* upon its removal, allowing for any observed significant difference to be attributed to differences in N-terminal acetylation. Nevertheless, the effects of the Protein-A tag on Ssa1 chaperone function and binding should be addressed in the future.

Because we were unable to co-purify endogenous co-chaperone with Ssa1-PrA in *S. cerevisiae*, we instead expressed and purified the Hsp40 co-chaperone, Ydj1, in an exogenous prokaryotic system. The purification of Ydj1 by IMAC was successful and the resulting yield was reasonably pure, as determined by SDS-PAGE and the mAU peak seen during the corresponding chromatograph, respectively (Figure 13a, Figure 13b). While we did not quantify the yield of co-chaperone attained by this purification method, the appearance of protein bands following Coomassie staining indicated that our eluted protein concentration was within a milligram range. While it is highly unlikely that a protein other than Ydj1 would be purified in high concentrations using this approach, we did not confirm the identity of our purified protein by Western blot. It still remains necessary to assess whether that the His-tag can be cleaved from the purified Ydj1, and that the co-chaperone is enzymatically active. These are all necessary steps before initiating Ssa1 co-chaperone binding studies. Acknowledging these limitations, the Ydj1 that is obtained by this purification is arguably sufficient for its intended use in future studies.

Understanding the various factors which contribute to chaperone function, efficiency, and mechanism is of great importance. This importance is only further

stressed after assessing the cooperative and dynamic relationships ongoing between the major chaperone families and their various co-chaperones in order to maintain proteostasis. Of the chaperone families, the need for the continued study of Hsp70 and its modification is emphasized when considering the apparent incongruity between the number of Hsp70-encoding genes and its numerous functional roles within the cell.

Prior to this study, the functional role of N-terminal acetylation in the context of Hsp70 chaperone activity has largely been overlooked, and previous purification methods used to obtain Hsp70 were relatively inaccessible due to their expensive, time-consuming and materialistic natures. This study established a highly efficient, one-step purification of Ssa1 that yields highly pure, enzymatically active chaperone that can be used to further elucidate the effects of N-terminal acetylation. Furthermore, this study has also taken the steps to establish the basis for evaluating the differences in Ssa1 chaperone activity that are attributable to N-terminal acetylation by purifying Ssa1 in N-terminal acetylation deficient backgrounds and confirming that WT Hsp70 is N-terminally acetylated by IEF. Through the expression and purification of Ydj1, this study has also provided the groundwork for future co-chaperone binding experiments, which will provide further insight to the contribution of N-terminal acetylation to Hsp70 chaperone activity and efficiency.

References

Abrams JL, Verghese J, Gibney PA, Morano KA. 2014. Hierarchical functional specificity of cytosolic heat shock protein 70 (Hsp70) nucleotide exchange factors in yeast. J Biol Chem. 289(19):13155–13167. doi:10.1074/jbc.M113.530014.

Affinity Chromatography: Vol II. [Internet].[Updated 2016, May]. GE Healthcare.; [cited 2018 May 8]. Available from: https://www.sigmaaldrich.com/content/dam/sigma-aldrich/docs/promo_NOT_INDEXED/General_Information/1/ge-affinity-chromatography.pdf

Ahmad, M. et al. (2014) Protein expression in *Pichia pastoris*: recent achievements and perspectives for heterologous protein production. Applications in Microbiology and Biotechnology. 98: 5301-5317.

Aksnes H, Hole K, Arnesen T. 2015. Chapter Seven - Molecular, Cellular, and Physiological Significance of N-Terminal Acetylation. In: Jeon KW, editor. International Review of Cell and Molecular Biology. Vol. 316. Academic Press. p. 267–305. http://www.sciencedirect.com/science/article/pii/S1937644815000027.

Ametzazurra A, Larrea E, Civeira MP, Prieto J, Aldabe R. 2008. Implication of human N-α-acetyltransferase 5 in cellular proliferation and carcinogenesis. Oncogene. 27(58):7296–7306. doi:10.1038/onc.2008.332.

Anderson JP, Walker DE, Goldstein JM, de Laat R, Banducci K, Caccavello RJ, Barbour R, Huang J, Kling K, Lee M, et al. 2006. Phosphorylation of Ser-129 Is the Dominant Pathological Modification of α-Synuclein in Familial and Sporadic Lewy Body Disease. Journal of Biological Chemistry. 281(40):29739–29752. doi:10.1074/jbc.M600933200.

Anfinsen CB. 1973. Principles that Govern the Folding of Protein Chains. Science. 181(4096):223–230.

Arnesen T, Anderson D, Baldersheim C, Lanotte M, Varhaug JE, Lillehaug JR. 2005. Identification and characterization of the human ARD1-NATH protein acetyltransferase complex. Biochem J. 386(Pt 3):433–443. doi:10.1042/BJ20041071.

Arnesen T, Van Damme P, Polevoda B, Helsens K, Evjenth R, Colaert N, Varhaug JE, Vandekerckhove J, Lillehaug JR, Sherman F, et al. 2009. Proteomics analyses reveal the evolutionary conservation and divergence of N-terminal acetyltransferases from yeast and humans. Proc Natl Acad Sci USA. 106(20):8157. doi:10.1073/pnas.0901931106.

Arnold RJ, Polevoda B, Reilly JP, Sherman F. 1999. The Action of N-terminal Acetyltransferases on Yeast Ribosomal Proteins. Journal of Biological Chemistry. 274(52):37035–37040. doi:10.1074/jbc.274.52.37035.

Aron R, Lopez N, Walter W, Craig EA, Johnson J. 2005. In vivo bipartite interaction between the Hsp40 Sis1 and Hsp70 in Saccharomyces cerevisiae. Genetics. 169(4):1873–1882. doi:10.1534/genetics.104.037242.

Barral JM, Broadley SA, Schaffar G, Hartl FU. 2004. Roles of molecular chaperones in protein misfolding diseases. Seminars in Cell & Developmental Biology. 15(1):17–29. doi:10.1016/j.semcdb.2003.12.010.

Blatch GL, Lässle M. 1999. The tetratricopeptide repeat: a structural motif mediating protein-protein interactions. BioEssays. 21(11):932–939. doi:10.1002/(SICI)1521-1878(199911)21:11<932::AID-BIES5>3.0.CO;2-N.

Boorstein W, Ziegelhoffer T, Craig EA. 1994. Molecular evolution of the Hsp70 multigene family. Journal of Molecular Evolution. 38:1–17. doi:10.1007/BF00175490.
Brasher MDR, Thorpe R. 1998. Isoelectric Focusing. In: Delves PJ, editor. Encyclopedia of Immunology (Second Edition). Oxford: Elsevier. p. 1510–1514. http://www.sciencedirect.com/science/article/pii/B0122267656003960.

Brasher MDR, Thorpe R. 1998. Isoelectric Focusing. In: Delves PJ, editor. Encyclopedia of Immunology (Second Edition). Oxford: Elsevier. p. 1510–1514. http://www.sciencedirect.com/science/article/pii/B0122267656003960.

Brower CS, Varshavsky A. 2009. Ablation of arginylation in the mouse N-end rule pathway: loss of fat, higher metabolic rate, damaged spermatogenesis, and neurological perturbations. PLoS One. 4(11):e7757–e7757. doi:10.1371/journal.pone.0007757.

Caesar R, Warringer J, Blomberg A. 2006. Physiological Importance and Identification of Novel Targets for the N-Terminal Acetyltransferase NatB. Eukaryot Cell. 5(2):368. doi:10.1128/EC.5.2.368-378.2006.

Cashikar AG, Duennwald M, Lindquist SL. 2005. A chaperone pathway in protein disaggregation. Hsp26 alters the nature of protein aggregates to facilitate reactivation by Hsp104. J Biol Chem. 280(25):23869–23875. doi:10.1074/jbc.M502854200.

Cheetham ME, Jackson AP, Anderton BH. 1994. Regulation of 70-kDa Heat-Shock-Protein ATPase Activity and Substrate Binding by Human DnaJ-Like Proteins, HSJ1a and HSJ1b. European Journal of Biochemistry. 226(1):99–107. doi:10.1111/j.1432-1033.1994.00t99.x.

Coleman CS, Huang H, Pegg AE. 1996. Structure and critical residues at the active site of spermidine/spermine-N1-acetyltransferase. Biochem J. 316(3):697–701. doi:10.1042/bj3160697.

Cyr DM, Lu X, Douglas MG. 1992. Regulation of Hsp70 function by a eukaryotic DnaJ homolog. Journal of Biological Chemistry. 267(29):20927–20931.

Cyr DM, Douglas MG. 1994. Differential regulation of Hsp70 subfamilies by the eukaryotic DnaJ homologue YDJ1. Journal of Biological Chemistry. 269(13):9798–9804.

Daugaard M, Rohde M, Jäättelä M. 2007. The heat shock protein 70 family: Highly homologous proteins with overlapping and distinct functions. FEBS Letters. 581(19):3702–3710. doi:10.1016/j.febslet.2007.05.039.

Eiyama A, Okamoto K. 2015. Protein N-terminal Acetylation by the NatA Complex Is Critical for Selective Mitochondrial Degradation. J Biol Chem. 290(41):25034–25044. doi:10.1074/jbc.M115.677468.

Fan C-Y, Ren H-Y, Lee P, Caplan AJ, Cyr DM. 2005. The Type I Hsp40 Zinc Finger-like Region Is Required for Hsp70 to Capture Non-native Polypeptides from Ydj1. Journal of Biological Chemistry. 280(1):695–702. doi:10.1074/jbc.M410645200.

Feifel B, Sandmeier E, Schönfeld HJ, Christen P. (1996) Potassium ion and the molecular-chaperone activity of DnaK. European Journal of Biochemistry 237: 318-321.

Forte GMA, Pool MR, Stirling CJ. 2011. N-Terminal Acetylation Inhibits Protein Targeting to the Endoplasmic Reticulum. PLOS Biology. 9(5):e1001073. doi:10.1371/journal.pbio.1001073.

Gautschi M, Just S, Mun A, Ross S, Rücknagel P, Dubaquié Y, Ehrenhofer-Murray A, Rospert S. 2003. The yeast N(alpha)-acetyltransferase NatA is quantitatively anchored to the ribosome and interacts with nascent polypeptides. Mol Cell Biol. 23(20):7403–7414. doi:10.1128/mcb.23.20.7403-7414.2003.

Geissenhöner A, Weise C, Ehrenhofer-Murray AE. 2004. Dependence of ORC silencing function on NatA-mediated N-alpha acetylation in Saccharomyces cerevisiae. Mol Cell Biol. 24(23):10300–10312. doi:10.1128/MCB.24.23.10300-10312.2004.

Giese KC, Basha E, Catague BY, Vierling E. 2005. Evidence for an essential function of the N terminus of a small heat shock protein *in vivo*, independent of *in vitro* chaperone activity. Proc Natl Acad Sci U S A. 102(52):18896–18901. doi:10.1073/pnas.0506169103.

Glover JR, Lindquist S. 1988. Hsp104, Hsp70, and Hsp40: A novel chaperone system that rescues previously aggregated proteins. Cell. 94(1):73–82. doi:10.1016/s0092-8674(00)81223-4.

Gong W, Hu W, Xu L, Wu H, Wu S, Zhang H, Wang J, Jones GW, Perrett S. 2018. The C-terminal GGAP motif of Hsp70 mediates substrate recognition and stress response in yeast. Journal of Biological Chemistry. 293(46):17663–17675. doi:10.1074/jbc.RA118.002691.

Greene MK, Maskos K, Landry SJ. 1998. Role of the J-domain in the cooperation of Hsp40 with Hsp70. Proc Natl Acad Sci USA. 95(11):6108. doi:10.1073/pnas.95.11.6108.

Griffith AA, Boutin J, Holmes W. 2018. A highly efficient, one-step purification of the Hsp70 chaperone Ssa1. Protein Expression and Purification. 152:56–63. doi:10.1016/j.pep.2018.07.006.

Griffith AA, Holmes WM. 2019. Fine Tuning: Effects of Post-Translational Modification on Hsp70 chaperones. International Journal of Molecular Sciences. 20(17):4207. doi:10.3390/ijms20174207.

Gupta RS, Golding GB. 1993. Evolution of Hsp70 gene and its implications regarding relationships between archaebacteria, eubacteria, and eukaryotes. Journal of Molecular Evolution. 37:573–582. doi:10.1007/BF0182743.

Hartl FU, Bracher A, Hayer-Hartl M. 2011. Molecular chaperones in protein folding and proteostasis. Nature. 475(7356):324–332. doi:10.1038/nature10317.

Hermann GJ, King EJ, Shaw JM. 1997. The yeast gene, MDM20, is necessary for mitochondrial inheritance and organization of the actin cytoskeleton. J Cell Biol. 137(1):141–153. doi:10.1083/jcb.137.1.141.

Hershko A, Heller H, Eytan E, Kaklij G, Rose IA. 1984. Role of the alpha-amino group of protein in ubiquitin-mediated protein breakdown. Proc Natl Acad Sci U S A. 81(22):7021–7025. doi:10.1073/pnas.81.22.7021.

Hoter A, El-Sabban ME, Naim HY. 2018. The HSP90 Family: Structure, Regulation, Function, and Implications in Health and Disease. Int J Mol Sci. 19(9):2560. doi:10.3390/ijms19092560.

Hu J, Wu Y, Li J, Qian X, Fu Z, Sha B. 2008. The crystal structure of the putative peptide-binding fragment from the human Hsp40 protein Hdj1. BMC Struct Biol. 8:3–3. doi:10.1186/1472-6807-8-3.

Hwang C-S, Shemorry A, Varshavsky A. 2010. N-terminal acetylation of cellular proteins creates specific degradation signals. Science. 327(5968):973–977. doi:10.1126/science.1183147.

Hydrophobic Interaction and Reversed Phase Chromatography: Principles and Methods. [Internet]. [Updated 2006]. GE Healthcare.; [Cited 2018 May 8] Available from: http://proteins.gelifesciences.com/~/media/protein-purification-ib/documents/handbooks/hydrophobic_interaction_chromatography.pdf?la=en

Ion Exchange Chromatography: Principles and Methods. [Internet]. [Updated 2016, January]. GE Healthcare.; [cited 2018b May 8]. Available from:

http://proteins.gelifesciences.com/knowledge-library/protein-handbooks/~/media/protein-purification-ib/documents/handbooks/ion_exchange_chromatography.pdf?la=en

Jäättelä M, Wissing D, Bauer PA, Li GC. 1992. Major heat shock protein Hsp70 protects tumor cells from tumor necrosis factor cytotoxicity. EMBO J. 11(10):3507–3512.

Jana NR, Tanaka M, Wang G, Nukina N. 2000. Polyglutamine length-dependent interaction of Hsp40 and Hsp70 family chaperones with truncated N-terminal huntingtin: their role in suppression of aggregation and cellular toxicity. Human Molecular Genetics. 9(13):2009–2018. doi:10.1093/hmg/9.13.2009.

Jaya N, Garcia V, Vierling E. 2009. Substrate binding site flexibility of the small heat shock protein molecular chaperones. Proc Natl Acad Sci U S A. 106(37):15604–15609. doi:10.1073/pnas.0902177106.

Jayaraj GG, Hipp MS, Hartl FU. 2020. Functional Modules of the Proteostasis Network. Cold Spring Harbor Perspectives in Biology. 12(1). doi:10.1101/cshperspect.a033951.

Johnson JL, Brown C. 2009. Plasticity of the Hsp90 chaperone machine in divergent eukaryotic organisms. Cell Stress Chaperones. 14(1):83–94. doi:10.1007/s12192-008-0058-9.

Kalvik TV, Arnesen T. 2013. Protein N-terminal acetyltransferases in cancer. Oncogene. 32(3):269–276. doi:10.1038/onc.2012.82.

Kellner R, Hofmann H, Barducci A, Wunderlich B, Nettels D, Schuler B. 2014. Single-molecule spectroscopy reveals chaperone-mediated expansion of substrate protein. Proc Natl Acad Sci USA. 111(37):13355. doi:10.1073/pnas.1407086111.

Kim H-K, Kim R-R, Oh J-H, Cho H, Varshavsky A, Hwang C-S. 2014. The N-terminal methionine of cellular proteins as a degradation signal. Cell. 156(1–2):158–169. doi:10.1016/j.cell.2013.11.031.

Kispal G, Sumegi B, Dietmeier K, Bock I, Gajdos G, Tomcsanyi T, Sandor A. 1993. Cloning and sequencing of a cDNA encoding *Saccharomyces cerevisiae* carnitine acetyltransferase. Use of the cDNA in gene disruption studies. Journal of Biological Chemistry. 268(3):1824–1829.

Klaips CL, Jayaraj GG, Hartl FU. 2018. Pathways of cellular proteostasis in aging and disease. The Journal of Cell Biology. 217(1):51–63. doi:https://doi.org/10.1083/JCB.201709072.

Kityk R, Kopp J, Mayer MP. 2018. Molecular Mechanism of J-Domain-Triggered ATP Hydrolysis by Hsp70 Chaperones. Molecular Cell. 69(2):227-237.e4. doi:10.1016/j.molcel.2017.12.003.

Kontaxi C, Piccardo P, Gill AC. 2017. Lysine-Directed Post-translational Modifications of Tau Protein in Alzheimer's Disease and Related Tauopathies. Front Mol Biosci. 4:56–56. doi:10.3389/fmolb.2017.00056.

Krzewska J, Langer T, Liberek K. 2001. Mitochondrial Hsp78, a member of the Clp/Hsp100 family in Saccharomyces cerevisiae, cooperates with Hsp70 in protein refolding. FEBS Letters. 489(1):92–96. doi:10.1016/S0014-5793(00)02423-6.

Labrou NE. 2014. Protein Purification: An Overview. In: Labrou NE, editor. Protein Downstream Processing: Design, Development and Application of High and Low-Resolution Methods. Totowa, NJ: Humana Press. p. 3–10. https://doi.org/10.1007/978-1-62703-977-2_1.

Laufen T, Mayer MP, Beisel C, Klostermeier D, Mogk A, Reinstein J, Bukau B. 1999. Mechanism of regulation of Hsp70 chaperones by DnaJ cochaperones. Proc Natl Acad Sci USA. 96(10):5452. doi:10.1073/pnas.96.10.5452.

Lee S, Sowa ME, Watanabe Y, Sigler PB, Chiu W, Yoshida M, Tsai FTF. 2003. The Structure of ClpB: A Molecular Chaperone that Rescues Proteins from an Aggregated State. Cell. 115(2):229–240. doi:10.1016/S0092-8674(03)00807-9.

Li GC, Li LG, Liu YK, Mak JY, Chen LL, Lee WM. 1991. Thermal response of rat fibroblasts stably transfected with the human 70-kDa heat shock protein-encoding gene. Proc Natl Acad Sci USA. 88(5):1681. doi:10.1073/pnas.88.5.1681.

Liszczak G, Goldberg JM, Foyn H, Petersson EJ, Arnesen T, Marmorstein R. 2013. Molecular basis for N-terminal acetylation by the heterodimeric NatA complex. Nat Struct Mol Biol. 20(9):1098–1105. doi:10.1038/nsmb.2636.

Litt M, Kramer P, LaMorticella DM, Murphey W, Lovrien EW, Weleber RG. 1998. Autosomal Dominant Congenital Cataract Associated with a Missense Mutation in the Human Alpha Crystallin Gene CRYAA. Human Molecular Genetics. 7(3):471–474. doi:10.1093/hmg/7.3.471.

Liu Q, Hendrickson WA. 2007. Insights into Hsp70 chaperone activity from a crystal structure of the yeast Hsp110 Sse1. Cell. 131(1):106–120. doi:10.1016/j.cell.2007.08.039.

Lu Z, Cyr DM. 1998. The Conserved Carboxyl Terminus and Zinc Finger-like Domain of the Co-chaperone Ydj1 Assist Hsp70 in Protein Folding. Journal of Biological Chemistry. 273(10):5970–5978. doi:10.1074/jbc.273.10.5970.

Magrané J, Smith RC, Walsh K, Querfurth HW. 2004. Heat shock protein 70 participates in the neuroprotective response to intracellularly expressed beta-amyloid in neurons. J Neurosci. 24(7):1700–1706. doi:10.1523/JNEUROSCI.4330-03.2004.

McLoughlin F, Basha E, Fowler ME, Kim M, Bordowitz J, Katiyar-Agarwal S, Vierling E. 2016. Class I and II Small Heat Shock Proteins Together with HSP101 Protect Protein Translation Factors during Heat Stress. Plant Physiol. 172(2):1221–1236. doi:10.1104/pp.16.00536.

Misselwitz B, Staeck O, Rapoport TA. 1998. J Proteins Catalytically Activate Hsp70 Molecules to Trap a Wide Range of Peptide Sequences. Molecular Cell. 2(5):593–603. doi:10.1016/S1097-2765(00)80158-6.

Mayer MP, Kityk R. 2015. Insights into the molecular mechanism of allostery in Hsp70s. Front Mol Biosci. 2:58–58. doi:10.3389/fmolb.2015.00058.

Morgner N, Schmidt C, Beilsten-Edmands V, Ebong I, Patel NA, Clerico EM, Kirschke E, Daturpalli S, Jackson SE, Agard D, et al. 2015. Hsp70 Forms Antiparallel Dimers Stabilized by Post-translational Modifications to Position Clients for Transfer to Hsp90. Cell Reports. 11(5):759–769. doi:10.1016/j.celrep.2015.03.063.

Mullen JR, Kayne PS, Moerschell RP, Tsunasawa S, Gribskov M, Colavito-Shepanski M, Grunstein M, Sherman F, Sternglanz R. 1989. Identification and characterization of genes and mutants for an N-terminal acetyltransferase from yeast. EMBO J. 8(7):2067–2075.

Needham PG, Patel HJ, Chiosis G, Thibodeau PH, Brodsky JL. 2015. Mutations in the Yeast Hsp70, Ssa1, at P417 Alter ATP Cycling, Interdomain Coupling, and Specific Chaperone Functions. J Mol Biol. 427(18):2948–2965. doi:10.1016/j.jmb.2015.04.010.

Needham, P.G., Masison D.C. (2008) Prion-impairing mutations in HSP70 chaperone SSA1: Effects on ATPase and chaperone activities. Arch Biochem Biophys. 478 (2): 167-174.

Ngosuwan J, Wang NM, Fung KL, Chirico WJ. 2003. Roles of Cytosolic Hsp70 and Hsp40 Molecular Chaperones in Post-translational Translocation of Presecretory Proteins into the Endoplasmic Reticulum. Journal of Biological Chemistry. 278(9):7034–7042. doi:10.1074/jbc.M210544200.

Ojha J, Karmegam RV, Masilamoni JG, Terry AV Jr, Cashikar AG. 2011. Behavioral Defects in Chaperone-Deficient Alzheimer's Disease Model Mice. PLOS ONE. 6(2):e16550. doi:10.1371/journal.pone.0016550.

Okuda M, Niwa T, Taguchi H. 2015. Single-molecule analyses of the dynamics of heat shock protein 104 (Hsp104) and protein aggregates. J Biol Chem. 290(12):7833–7840. doi:10.1074/jbc.M114.620427.

Osberg C, Aksnes H, Ninzima S, Marie M, Arnesen T. 2016. Microscopy-based *Saccharomyces cerevisiae* complementation model reveals functional conservation and

redundancy of N-terminal acetyltransferases. Scientific Reports. 6(1):31627. doi:10.1038/srep31627.

Park EC, Szostak JW. 1992. ARD1 and NAT1 proteins form a complex that has N-terminal acetyltransferase activity. EMBO J. 11(6):2087–2093.

Pelham HR. 1984. Hsp70 accelerates the recovery of nucleolar morphology after heat shock. EMBO J. 3(13):3095–3100.

Persson B, Flinta C, von Heijne G, Jörnvall H. 1985. Structures of N-terminally acetylated proteins. European Journal of Biochemistry. 152(3):523–527. doi:10.1111/j.1432-1033.1985.tb09227.x.

Peschek J, Braun N, Rohrberg J, Back KC, Kriehuber T, Kastenmüller A, Weinkauf S, Buchner J. 2013. Regulated structural transitions unleash the chaperone activity of αB-crystallin. Proc Natl Acad Sci U S A. 110(40):E3780–E3789. doi:10.1073/pnas.1308898110.

Petrescu AJ, Calmettes P, Durand D, Receveur V, Smith JC. 2000. Change in backbone torsion angle distribution on protein folding. Protein Sci. 9(6):1129–1136. doi:10.1110/ps.9.6.1129.

Pezza JA, Langseth SX, Raupp Yamamoto R, Doris SM, Ulin SP, Salomon AR, Serio TR. 2009. The NatA acetyltransferase couples Sup35 prion complexes to the [PSI+] phenotype. Mol Biol Cell. 20(3):1068–1080. doi:10.1091/mbc.e08-04-0436.

Polevoda B, Cardillo TS, Doyle TC, Bedi GS, Sherman F. 2003. Nat3p and Mdm20p Are Required for Function of Yeast NatB Nα-terminal Acetyltransferase and of Actin and Tropomyosin. Journal of Biological Chemistry. 278(33):30686–30697. doi:10.1074/jbc.M304690200.

Polevoda B, Norbeck J, Takakura H, Blomberg A, Sherman F. 1999. Identification and specificities of N-terminal acetyltransferases from *Saccharomyces cerevisiae*. EMBO J. 18(21):6155–6168. doi:10.1093/emboj/18.21.6155.

Polevoda B, Sherman F. 2000. Nα-terminal Acetylation of Eukaryotic Proteins. Journal of Biological Chemistry. 275(47):36479–36482. doi:10.1074/jbc.R000023200.

Polevoda B, Sherman F. 2001. NatC Nα-terminal Acetyltransferase of Yeast Contains Three Subunits, Mak3p, Mak10p, and Mak31p. Journal of Biological Chemistry. 276(23):20154–20159. doi:10.1074/jbc.M011440200.

Polevoda B, Sherman F. 2002. The diversity of acetylated proteins. Genome Biology. 3(5):reviews0006.1. doi:10.1186/gb-2002-3-5-reviews0006.

Poulain P, Gelly J-C, Flatters D. 2010. Detection and Architecture of Small Heat Shock Protein Monomers. PLOS ONE. 5(4):e9990. doi:10.1371/journal.pone.0009990.

Prodromou C, Panaretou B, Chohan S, Siligardi G, O'Brien R, Ladbury JE, Roe SM, Piper PW, Pearl LH. 2000. The ATPase cycle of Hsp90 drives a molecular "clamp" via transient dimerization of the N-terminal domains. EMBO J. 19(16):4383–4392. doi:10.1093/emboj/19.16.4383.

Prodromou C, Roe SM, O'Brien R, Ladbury JE, Piper PW, Pearl LH. 1997. Identification and Structural Characterization of the ATP/ADP-Binding Site in the Hsp90 Molecular Chaperone. Cell. 90(1):65–75. doi:10.1016/S0092-8674(00)80314-1.

Rippmann F, Taylor WR, Rothbard JB, Green NM. 1991. A hypothetical model for the peptide binding domain of hsp70 based on the peptide binding domain of HLA. EMBO J. 10(5):1053–1059.

Rosenzweig R, Nillegoda NB, Mayer MP, Bukau B. 2019. The Hsp70 chaperone network. Nature Reviews Molecular Cell Biology. 20(11):665–680. doi:10.1038/s41580-019-0133-3.

Rüdiger S, Germeroth L, Schneider-Mergener J, Bukau B. 1997. Substrate specificity of the DnaK chaperone determined by screening cellulose-bound peptide libraries. EMBO J. 16(7):1501–1507. doi:10.1093/emboj/16.7.1501.

Rutsdottir G, Härmark J, Weide Y, Hebert H, Rasmussen MI, Wernersson S, Respondek M, Akke M, Højrup P, Koeck PJB, et al. 2017. Structural model of dodecameric heat-shock protein Hsp21: Flexible N-terminal arms interact with client proteins while C-terminal tails maintain the dodecamer and chaperone activity. J Biol Chem. 292(19):8103–8121. doi:10.1074/jbc.M116.766816.

Sha B, Lee S, Cyr DM. 2000. The crystal structure of the peptide-binding fragment from the yeast Hsp40 protein Sis1. Structure. 8(8):799–807. doi:10.1016/S0969-2126(00)00170-2.

Shaner L, Wegele H, Buchner J, Morano KA. 2005. The Yeast Hsp110 Sse1 Functionally Interacts with the Hsp70 Chaperones Ssa and Ssb. Journal of Biological Chemistry. 280(50):41262–41269. doi:10.1074/jbc.M503614200.

Sharma D, Martineau CN, Le Dall M-T, Reidy M, Masison DC, Kabani M. 2009. Function of SSA subfamily of Hsp70 within and across species varies widely in complementing Saccharomyces cerevisiae cell growth and prion propagation. PLoS One. 4(8):e6644–e6644. doi:10.1371/journal.pone.0006644.

Shemorry A, Hwang CS, Varshavsky A. 2013. Control of protein quality and stoichiometries by N-terminal acetylation and the N-end rule pathway. Mol Cell. 50(4):540–551. doi:10.1016/j.molcel.2013.03.018.

Shorter J, Lindquist S. 2008. Hsp104, Hsp70 and Hsp40 interplay regulates formation, growth and elimination of Sup35 prions. EMBO J. 27(20):2712–2724. doi:10.1038/emboj.2008.194.

Singer JM, Shaw JM. 2003. Mdm20 protein functions with Nat3 protein to acetylate Tpm1 protein and regulate tropomyosin-actin interactions in budding yeast. Proc Natl Acad Sci U S A. 100(13):7644–7649. doi:10.1073/pnas.1232343100.

Size exclusion chromatography: Principles and Methods. [Internet]. [Updated 2000, December]. GE Healthcare.; [cited 2018c May 8]. Available from: http://proteins.gelifesciences.com/~/media/protein-purification-ib/documents/handbooks/size-exclusion-chromatography-handbook.pdf?la=en

Sondermann H, Scheufler C, Schneider C, Höhfeld J, Hartl FU, Moarefi I. 2001. Structure of a Bag/Hsc70 Complex: Convergent Functional Evolution of Hsp70 Nucleotide Exchange Factors. Science. 291(5508):1553. doi:10.1126/science.1057268.

Sullivan W, Stensgard B, Caucutt G, Bartha B, McMahon N, Alnemri ES, Litwack G, Toft D. 1997. Nucleotides and Two Functional States of hsp90. Journal of Biological Chemistry. 272(12):8007–8012. doi:10.1074/jbc.272.12.8007.

Taneva SG, Moro F, Velázquez-Campoy A, Muga A. 2010. Energetics of Nucleotide-Induced DnaK Conformational States. Biochemistry. 49(6):1338–1345. doi:10.1021/bi901847q.

Treweek TM, Rekas A, Lindner RA, Walker MJ, Aquilina JA, Robinson CV, Horwitz J, Der Perng M, Quinlan RA, Carver JA. 2005. R120G αB-crystallin promotes the unfolding of reduced α-lactalbumin and is inherently unstable. The FEBS Journal. 272(3):711–724. doi:10.1111/j.1742-4658.2004.04507.x.

Truman AW, Kristjansdottir K, Wolfgeher D, Ricco N, Mayampurath A, Volchenboum SL, Clotet J, Kron SJ. 2015. Quantitative proteomics of the yeast Hsp70/Hsp90 interactomes during DNA damage reveal chaperone-dependent regulation of ribonucleotide reductase. J Proteomics. 112:285–300. doi:10.1016/j.jprot.2014.09.028.

Turoverov KK, Keznetsova IM, Uversky VN. 2010. The Protein Kingdom Extended: Ordered and Intrinsically Disordered Proteins, Their Folding, Supramolecular Complex Formation, and Aggregation. Prog Biophys Mol Biol. 102(2):73–84.

Umehara K, Hoshikawa M, Tochio N, Tate S-I. 2018. Substrate Binding Switches the Conformation at the Lynchpin Site in the Substrate-Binding Domain of Human Hsp70 to Enable Allosteric Interdomain Communication. Molecules. 23(3):528. doi:10.3390/molecules23030528.

Vacher C, Garcia-Oroz L, Rubinsztein DC. 2005. Overexpression of yeast hsp104 reduces polyglutamine aggregation and prolongs survival of a transgenic mouse model of Huntington's disease. Human Molecular Genetics. 14(22):3425–3433. doi:10.1093/hmg/ddi372.

Van Damme P, Hole K, Pimenta-Marques A, Helsens K, Vandekerckhove J, Martinho RG, Gevaert K, Arnesen T. 2011. NatF contributes to an evolutionary shift in protein N-terminal acetylation and is important for normal chromosome segregation. PLoS Genet. 7(7):e1002169–e1002169. doi:10.1371/journal.pgen.1002169.

Van Damme P, Lasa M, Polevoda B, Gazquez C, Elosegui-Artola A, Kim DS, De Juan-Pardo E, Demeyer K, Hole K, Larrea E, et al. 2012. N-terminal acetylome analyses and functional insights of the N-terminal acetyltransferase NatB. Proc Natl Acad Sci USA. 109(31):12449. doi:10.1073/pnas.1210303109.

Van Damme P, Støve SI, Glomnes N, Gevaert K, Arnesen T. 2014. A Saccharomyces cerevisiae model reveals in vivo functional impairment of the Ogden syndrome N-terminal acetyltransferase NAA10 Ser37Pro mutant. Mol Cell Proteomics. 13(8):2031–2041. doi:10.1074/mcp.M113.035402.

van der Weerd L, Tariq Akbar M, Aron Badin R, Valentim LM, Thomas DL, Wells DJ, Latchman DS, Gadian DG, Lythgoe MF, de Belleroche JS. 2009. Overexpression of Heat Shock Protein 27 Reduces Cortical Damage after Cerebral Ischemia. J Cereb Blood Flow Metab. 30(4):849–856. doi:10.1038/jcbfm.2009.249.

Varshavsky A. 2011. The N-end rule pathway and regulation by proteolysis. Protein Sci. 20(8):1298–1345. doi:10.1002/pro.666.

Vicart P, Caron A, Guicheney P, Li Z, Prévost M-C, Faure A, Chateau D, Chapon F, Tomé F, Dupret J-M, et al. 1998. A missense mutation in the αB-crystallin chaperone gene causes a desmin-related myopathy. Nature Genetics. 20(1):92–95. doi:10.1038/1765.

Vjestica A, Zhang D, Liu J, Oliferenko S. 2013. Hsp70-Hsp40 chaperone complex functions in controlling polarized growth by repressing Hsf1-driven heat stress-associated transcription. PLoS Genet. 9(10):e1003886–e1003886. doi:10.1371/journal.pgen.1003886.

Wall D, Zylicz M, Georgopoulos C. 1995. The Conserved G/F Motif of the DnaJ Chaperone Is Necessary for the Activation of the Substrate Binding Properties of the DnaK Chaperone. Journal of Biological Chemistry. 270(5):2139–2144. doi:10.1074/jbc.270.5.2139.

Wang L, Xie C, Greggio E, Parisiadou L, Shim H, Sun L, Chandran J, Lin X, Lai C, Yang W-J, et al. 2008. The chaperone activity of heat shock protein 90 is critical for

maintaining the stability of leucine-rich repeat kinase 2. J Neurosci. 28(13):3384–3391. doi:10.1523/JNEUROSCI.0185-08.2008.

Warrick JM, Chan HYE, Gray-Board GL, Chai Y, Paulson HL, Bonini NM. 1999. Suppression of polyglutamine-mediated neurodegeneration in *Drosophila* by the molecular chaperone HSP70. Nature Genetics. 23(4):425–428. doi:10.1038/70532.

Wegele H, Haslbeck M, Buchner J. 2003. Recombinant expression and purification of Ssa1p (Hsp70) from Saccharomyces cerevisiae using *Pichia pastoris*. Journal of Chromatography B. 786(1):109–115. doi:10.1016/S1570-0232(02)00724-9.

Wegele H, Haslbeck M, Reinstein J, Buchner J. 2003. Sti1 Is a Novel Activator of the Ssa Proteins. Journal of Biological Chemistry. 278(28):25970–25976. doi:10.1074/jbc.M301548200.

Weibezahn J, Tessarz P, Schlieker C, Zahn R, Maglica Z, Lee S, Zentgraf H, Weber-Ban EU, Dougan DA, Tsai FTF, et al. 2004. Thermotolerance Requires Refolding of Aggregated Proteins by Substrate Translocation through the Central Pore of ClpB. Cell. 119(5):653–665. doi:10.1016/j.cell.2004.11.027.

Wenzlau Janet M., Garl Pamela J., Simpson Peter, Stenmark Kurt R., West James, Artinger Kristin B., Nemenoff Raphael A., Weiser-Evans Mary C.M. 2006. Embryonic Growth-Associated Protein Is One Subunit of a Novel N-Terminal Acetyltransferase Complex Essential for Embryonic Vascular Development. Circulation Research. 98(6):846–855. doi:10.1161/01.RES.0000214539.86593.7a.

Wilbanks SM, McKay DB. (1995) How Potassium Affects the activity of the molecular chaperone Hsc70. Journal of Biological Chemistry 270: 2251-2257.

Zeymer C, Werbeck ND, Schlichting I, Reinstein J. 2013. The molecular mechanism of Hsp100 chaperone inhibition by the prion curing agent guanidinium chloride. J Biol Chem. 288(10):7065–7076. doi:10.1074/jbc.M112.432583.

Zhang P, Leu JI-J, Murphy ME, George DL, Marmorstein R. 2014. Crystal Structure of the Stress-Inducible Human Heat Shock Protein 70 Substrate-Binding Domain in Complex with Peptide Substrate. PLOS ONE. 9(7):e103518. doi:10.1371/journal.pone.0103518.

Żwirowski S, Kłosowska A, Obuchowski I, Nillegoda NB, Piróg A, Ziętkiewicz S, Bukau B, Mogk A, Liberek K. 2017. Hsp70 displaces small heat shock proteins from aggregates to initiate protein refolding. EMBO J. 36(6):783–796. doi:10.15252/embj.201593378.

Zybailov B, Rutschow H, Friso G, Rudella A, Emanuelsson O, Sun Q, van Wijk KJ. 2008. Sorting Signals, N-Terminal Modifications and Abundance of the Chloroplast Proteome. PLOS ONE. 3(4):e1994. doi:10.1371/journal.pone.0001994.